Development of a multiparametric Optical Computed Tomography system for the study of biological samples

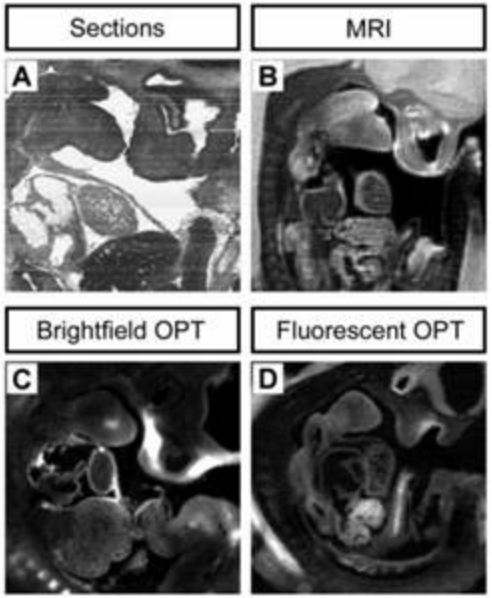

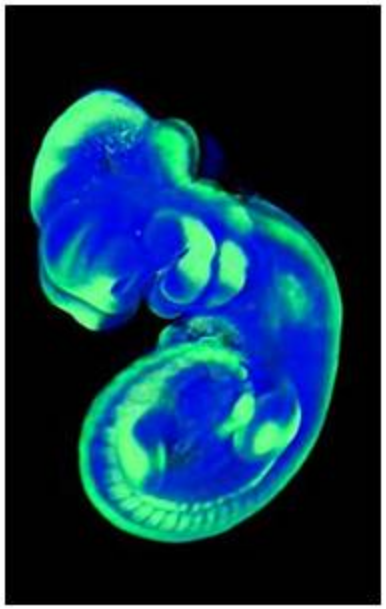

Michail Loizos, 4214
University of Crete, Physics Department

Contents

Chapter 1

X-rays, Computed Tomography to Optical Projection Tomography

1.1 Discovery of x-rays

1.1.1 Crooke's Tube

One of the most important steps for the evolution of diagnostic systems was the accidental discovery of X-rays by the German physicist Wilhelm Conrad Röentgen in 1895. Meanwhile, Röentgen was experimenting in his lab, trying to investigate the rays that were coming out from the Crooke's tube that he had. Crookes tube is an electric bulb made by glass. It contains 2 electrodes in partial vacuum, an anode and a cathode as seen in figure 1.1. When Voltage is applied, electrons travel from the cathode to the anode. The low pressure gas molecules inside the tube collide with the electrons so they become positively charged ions.These ions are attracted to the cathode,resulting to freeing more electrons from the cathode producing cathode rays .When electrons collide with glass atoms they fluoresce.

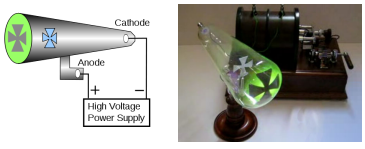

(a) (b)

Figure 1.1: A schematic presentation of Crooke's tube (a) and fluorescence using a cross-shaped anode (b). [2]

1.1.2 Röentgen's Experiment

Röentgen's research was focused on passing voltage through vacuum tubes. Electrons inside a Crooke's tube can be accelerated to high velocities. For instance , an applied voltage of 10kV can accelerate electrons up to a velocity of 20 percent the speed of light. On November 8^{th} in 1895, Röentgen was preparing to start a new session of experiments. For this purpose, he darkened his laboratory to observe the fluorescence from the cathode rays to make sure that the tube was receiving electricity. After he covered the tube with black cardboard . When he electrified the tube again, he noticed a slight glow coming from an object a few meters away.The object was a piece of paper which was coated with barium platinocyanide.Röentgen wasn't sure if rays could make it that far , so he repeated the experiment several times.The result was the same so this made him realize that the energy coming from the tube was responsible for this glow.

After his discovery, Röentgen continued his experiment for several weeks to discover the properties of this new type of energy. He noticed that when he placed his hand between the tube and the paper, he would see his bones glowing on the paper. Without being sure, he called his wife Bertha to show her his discovery. He placed her wife's hand under the tube and produced a static image of her hand.During that time, the idea of seeing the inside parts of the human body seemed to be pure imagination. Röentgen decided to inform his colleagues about his discovery. He named this form of energy X-rays. On December 28^{th} in 1895, Röentgen submitted a paper on his research. He named his article "On a new kind of Rays". His work became known to the world and brought excitement to the medical community. In 1901 he was rewarded with a Nobel Prize in Physics.

(a) W.C. Röentgen,1845-1923 (b) Röentgen's wife hand

Figure 1.2: Picture of W.C. Röentgen (a) and picture of Röentgen's wife hand (b), this is the first radiograph ever

1.2 X-rays

1.2.1 Definition and Shell theory

Nowdays, we know a lot more about X-rays. X-rays are electromagnetic waves of high energy and very short wavelength. The wavelength ranges from 0.1 to 100 Å, which means that they can penetrate inside atoms. X-rays have enough energy to ionize atoms,meaning they can rip off electrons from them.

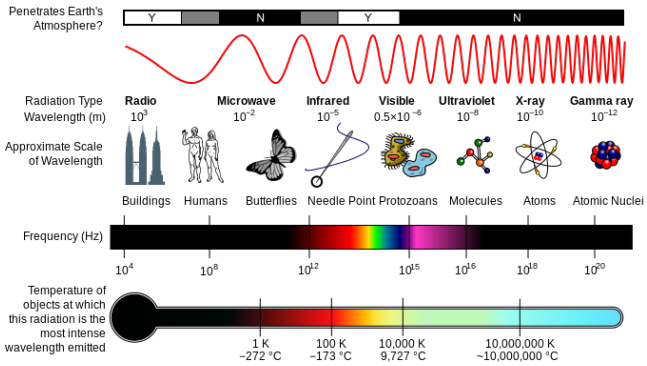

Figure 1.3: The electromagnetic spectrum with a frequency,temperature and a wavelength scale compared to everyday life objects.

The atom consists of a nucleus of protons and neutrons with electrons moving around them in orbitals.These orbits are called shells. A shell contains all electrons with the same principal quantum number n.The shells are K(2 electrons),L(8e),M(18e) and N(32e). Shells close to the nucleus have a bigger binding energy.X-rays can be produced by shooting electrons in a metal target under high voltage. There are two types of rays produced by this process. The first is characteristic x-rays. They are the trace of every atom because they emit in specific frequencies which differ from atom to atom. When a ray electron strikes a bound electron, it pushes it outside the atom creating a gap. This gap is filled by another electron of an outer shell which jumps from its higher energy level to the lower one where the electron is gone. A photon is emitted with energy equal the energy difference of these two levels. The spectrum of characteristic x-rays is discrete.The other type is Bremsstrahlung in German, or "braking radiation" in English. This is radiation caused by the scattering of an electron from another one or from an atomic nucleus. The moving electron loses kinetic energy and decelerates , emitting light as a result of the conservation of energy. The Bremsstrahlung radiation has a continuous spectrum.

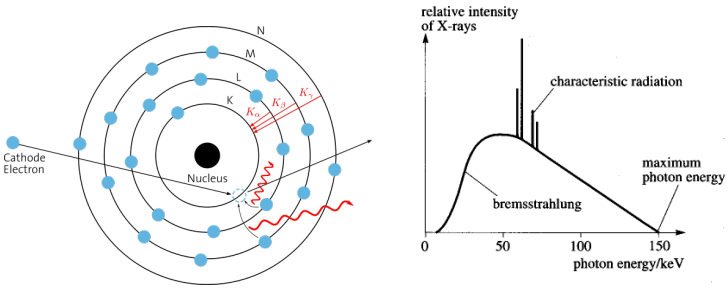

(a) Scheme of the x-ray mechanism (b) X-ray emission spectrum

Figure 1.4: A scheme of the x-ray mechanism (a) .K_α and K_β are the characteristic discrete emission lines seen in the x-ray spectrum.The indices α, β and γ are spectroscopic notations for different shell transitions (b) emission spectrum of x-rays.

1.2.2 Interaction with matter

There are 3 possible ways for x-rays to interact with matter: a) Photoelectric effect, b) Compton effect , c) pair production

Photoelectric effect is the emission of electrons when light strikes on a material. It was discovered initially by Heinrich Rudolf Hertz (1857-1894) in 1887. He noticed that when UV light strikes two metal electrodes with voltage applied between them, the voltage when the sparkle takes place is different. Later in 1902 Lenard pointed out the link between electricity and light and the concept of electron emission from metals. However, classic electromagnetic theory fails to explain the photoelectric effect because of the following arguments: a) The maximum kinetic energy of the electrons depend on the wavelength of the incoming radiation and not from its intensity. According to classic theory, electromagnetic waves consist of an oscillating electric and magnetic field and have an amplitude, with intensity depending as the square of the amplitude, so someone expects kinetic energy to be dependent from intensity. b) The emission of electrons is simultaneous with radiation incidence. c) The existence of an upper limit to the wavelength of the incoming radiation. These facts led Einstein to construct a new theory of light which consists of small discrete packets of energy. These quanta of light (photons) have an energy

$$E = h \cdot f \tag{1.2.1}$$

h is Planck constant and f is the frequency of radiation.

Furthemore, Einstein proposed the photoelectric equation which is able to solve all above problems for the photoelectric effect:

$$K_{max} = h \cdot f - W \tag{1.2.2}$$

where K_{max} is the maximum kinetic energy an electron can have when it escapes from the metal,$h \cdot f$ is the energy of the incoming radiation and W is the work function, the energy required for electrons in the outer energy levels of the metal to escape from it with zero kinetic energy . From this equation it can be seen that the maximum kinetic energy of the electrons is proportional with the frequency of radiation and there is an upper limit for the wavelength to observe the photoelectric effect . This limit is calculated if we demand $h \cdot f \geq W$

Compton effect is the scattering of photons by charged particles. Oftentimes scattering is caused by electrons. Compton scattering is inelastic, which means photons lose kinetic energy. The scattered radiation has a bigger wavelength than the initial because of the decrease in energy.Arthur H. Compton noticed that when he sent monochromatic x-rays to a graphite target, the scattered rays had a bigger wavelength. Once again, classic theory could not explain this change in frequency because it doesn't take into account light-particle duality.The wavelength shift can be calculated with combination of energy and momentum conservation. The result gives the following equation:

$$\lambda' - \lambda = \frac{h}{mc} \cdot (1 - cos\theta) \tag{1.2.3}$$

where λ' is the wavelength of scattered radiation, λ is the wavelength of the incoming radiation,h is planck constant, c the speed of light , m the mass of the scatter (usually electrons) and θ the scattering angle.

Finally, pair production is the creation of a particle-antiparticle pair, for example from a photon an electron-positron pair can be generated.In order for pair production to occur, energy provided must be at least equal or greater than the sum of the rest energies of the particles.For example, for electron-positron pair energy must be at least 1,022 MeV or greater.For lower energies between the range 1-500 keV, Compton and photoelectric effect are dominant. This process is seen in medicine in the PET scanner (positron emission tomography).

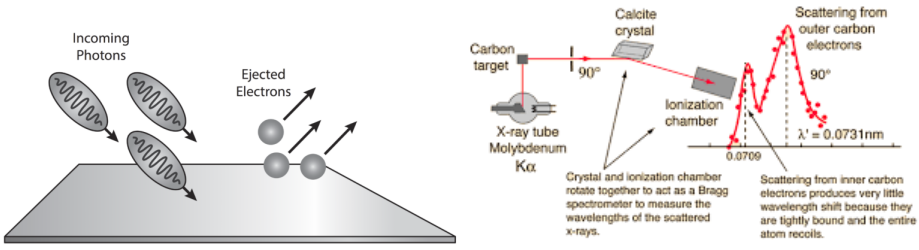

(a) (b)

Figure 1.5: a) Scheme of Photoelectric effect b) Experimental setup to observe Compton effect

A very important issue(especially in medicine) while dealing with x-rays is their attenuation from matter.When x-rays pass through matter, their in-

tensity decreases.This happens due to absorption and scattering combined together.Absorption of x-rays depends from 2 factors:

- The thickness x of the material
- The attenuation coefficient μ

When x-rays penetrate a material of thickness x with initial intensity I_0, the intensity decreases by dI.The thicker the material , the bigger the decrease in intensity because rays have a lot more time to interact with material atoms.Therefore, intensity and material thickness will be proportional with a constant μ, the attenuation coefficient. This is expressed mathematically as follows:

$$dI = -I \cdot \mu \cdot x \tag{1.2.4}$$

integration gives

$$I = I_0 \cdot e^{-\mu \cdot x} \tag{1.2.5}$$

When radiation penetrates a material , the degree of attenuation (absorption and scattering) depends on the density (how many atoms are present in the material) and the cross section (how often rays meet an atom inside the material).The attenuation coefficient has dimensions $length^{-1}$ and it's given from the following expression:

$$\mu = n \cdot \sigma \tag{1.2.6}$$

or

$$\mu = \frac{\sigma \cdot \rho \cdot N_A}{A} \tag{1.2.7}$$

, where σ is the cross section,ρ is the density of the material, N_A is Avogadro's number and A is the atomic weight

The attenuation coefficient μ for a two-dimensional distribution can be generalized as

$$\int_{ray} \mu(x, y)\, dx\, dy \tag{1.2.8}$$

1.3 Medical use of X-rays

The discovery of x-rays led the way for the invention of imaging systems in medicine. After Röentgen's experiments, during early 1896,X-rays were used to diagnose bone fractures and to treat gunshot wounds .A year after, William Morton used x-rays to take the first picture of a whole skeleton. The idea of having X-ray photos from the inside of human body without any kind of surgical intervention became of crucial importance. Until 1901, X-rays have become an important tool as it comes to clinical treatment. At that time hospitals where growing both in size and complexity and there were many attempts to improve both equipment and examination techniques. The use of X-rays was growing beyond observing fractures. They were used for detecting inflammations and

gallstones. Furthemore, doctors were able to detect the early stages of pulmonary tuberculosis, one of the top common death causes in the world at that time.

Later on, the quality of x-ray images improved so much that they could even show soft tissues.Additionally, with the injection of special contrast agents inside a patient's bloodstream it became possible to have a look at the vascular system.Thomas Alva Edison (1847-1931) contributed a lot to the development of medical imaging techniques. He among others improved the design of X-ray tubes. Hermann Von Helmholtz (1821-1894) studied the properties of x-rays and worked on the equations describing them, while measuring their ability to penetrate inside different materials. The branch of medicine that uses imaging to detect diseases is called radiology. There are various types of radiology techniques used for imaging: 1) Plain x-rays. 2) Fluoroscopy, 3) Magnetic Resonance imaging (MRI), 4) Mammography , 5) Nuclear Medicine, 6) Positron Emission Tomography(PET) and 7) Ultrasounds.

1.4 Computed Tomography

Computed Tomography is an imaging technique used to diagnose a disease. The word tomography comes from the Greek work "tomos" . The first idea that gave room for the invention of C.T came in 1917 with the mathematical theory of Radon's transform. The first computed tomographer ever was built in 1971 by Godfrey Hounsfield and was designed to take only pictures of a brain. Later in 1975 a full body Computed tomographer was built. During 1979 Hounsfield was rewarded with Nobel Prize in Physiology/Medicine for his invention.

The procedure of a CT scan is done by using an x-ray source which rotates around the patient. X-rays penetrate the patient's body and the produced signal is being analyzed using a computer.The use of the right algorithm can give cross-sectional images of a patient's parts. The obtained images are called slices. A combination of these slices can give a 3D image of the examined area.

Figure 1.6: Actual CT image of a head

1.5 From Computed Tomography to Optical Projection Tomography

Optical Projection Tomography is an imaging tool that can be used to image samples in 3D. It works with the same logic as CT. It produces a reconstructed,3D volume of the sample from projections from several angles but with the use of visible light , instead of ionizing radiation (X-rays).In optical projection tomography, the examined sample rotates instead of the x-ray source and the detector around the patient as in Computed Tomography.For the purpose of this project, two different measurement geometries will be used: Transmission and reflection.Transmission is used for absorption measurements and reflection is used for fluorescence measurements.

This method is ideal to measure samples in the scale of a few millimeters (or several microns) and can offer detailed images of biological tissues and gene expressions.This is the main reason the method is used in biomedical applications.The technique is linked also with microscopy methods.It fills the gap between confocal laser scanning microscopy and MRI in terms of scale.The problem with MRI is that when resolution is increased, the magnets used must be stronger, so the technique becomes too expensive to run in a lab. Also,it cannot provide image for histological stains and other protocols in order to give image for RNA expression patterns.One can rely on MRI for sample diameters on the order of a centimeter .Confocal laser microscopy can give clear, 3D images of objects using fluorochromes. It works best in the scale of hundreds of microns or less. Nevertheless,there is a restriction with O.P.T: The sample must be transparent or semi-transparent or in general it must allow a portion of light to transmit through it in order to obtain information from image reconstruction

Chapter 2

Tomographic 3D Volume Reconstruction

2.1 A review of the Tomographic Reconstruction problem

Tomography in general is a purely mathematical problem.Before getting into the mathematics of the reconstruction algorithm, the concepts that will be represented are described .Computed Tomography or OPT are used for 3D imaging. In order to do this, a proper mathematical theory must be constructed. The target is to apply this theory algorithmically in order to obtain the result. The first step was done by Johann Radon in 1917 with the concept of Radon Transform, which is the base of reconstructing a 3D image from projections.Another central idea for tomography is the Fourier slice theorem.

The main target of Tomography is to reconstruct the object volume by scanning back the projections through the object.Suppose that someone wants to map the exact location of an area, for example the two trees seen in figure 2.1. This mapping will be performed by having as the only data pictures from different orientations, for example east and south view. So the problem is to map the exact location of the trees by knowing the east and south view.This could be done by drawing lines from each tree for every direction and meet the intersections.This is somehow close to a tomography problem, with the difference that there are many more pictures, meaning more angles and also intensity is another parameter.The mission is to estimate the 3D volume of the area of interest by having pictures from several different angles. These pictures are called projections.These projections "return" back to the object with a procedure called filtered back projection,and produce 2D slices. If these slices are stacked together, the 3D Volume is obtained.

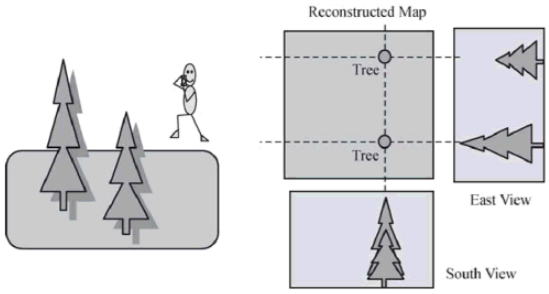

Figure 2.1: Every-day life analog for CT reconstruction problem [14]

2.2 Radon Transform and Projections

Mathematically, every captured image can be seen as a projection.A single projection is a set of line integrals of the object along straight ,parallel rays passing through the object.These lines are parameterized. A line integral in tomography represents the two-Dimensional profile of the attenuation coefficient when x-rays or visible light propagate along straight lines through the sample. The object can be modeled as a 2D function $f(x, y)$. The line integral is calculated for an angle θ along a line named L .Assume that parameterization variable is called t for the following analysis. This line integral can be calculated as follows:

$$P_\theta(t) = \int_{L(\theta,t)} f(x, y)ds \tag{2.2.1}$$

. This line integral $P_\theta(t)$ is also called the Radon Transform of the f(x,y) function.

$$P_\theta(t) = \int_{-\infty}^{+\infty}\int_{-\infty}^{+\infty} \delta(x \cdot cos\theta + y \cdot sin\theta - t) f(x, y)\, dx\, dy \tag{2.2.2}$$

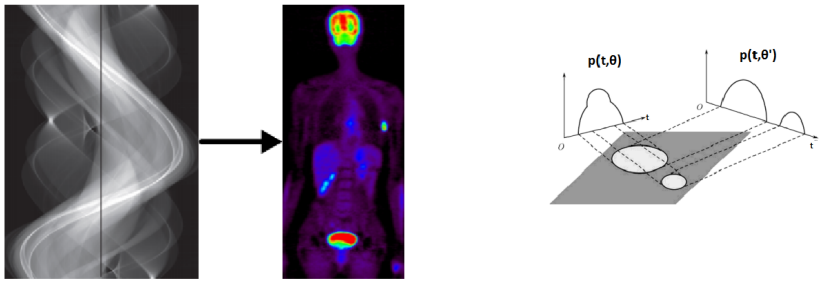

(a) (b)

Figure 2.2: a) Sinogram and b) Projections. [15]

Where delta function is zero everywhere except in the line L. Oftentimes Radon transform is also called a sinogram. A sinogram is basically an intensity distribution of projections on the $t-\theta$ plane. The term "sinogram" is used because this distribution is sinusoidal.

This theoretical model is correct but there is a problem: The limits on the integrals are infinite where all scans contain a finite number of projections. Also, analysis is performed in computers where all procedures are performed using memory bins. A more realistic approach is the use of the discrete Radon Transform:

$$P_i(t) = \int_{-\frac{\delta t}{2}}^{+\frac{\delta t}{2}} Rf(\theta, t+t')\, dt' \tag{2.2.3}$$

, where

$$R = \int_{\theta,t} f(x,y)dxdy \tag{2.2.4}$$

and δt is the width of the detector

Another realistic analog is this:Imagine every pixel of the image as matrix elements of a matrix.Every pixel has a linear density and every line passing through the object has a specific length including some pixels,until it reaches the detector.Also the detector can be modeled as discrete detector bins. This is close to how the Radon function work in matlab. Mathematically, a projection can be calculated as follows:

$$P(i,\theta) = \sum_{i=1}^{N}\sum_{j=1}^{N} a_{ij}x_j \tag{2.2.5}$$

, where x_j is the linear density of each pixel and a_{ij} the length of each line passing through the object incuding a number of pixels until it reaches the detector, for N pixels

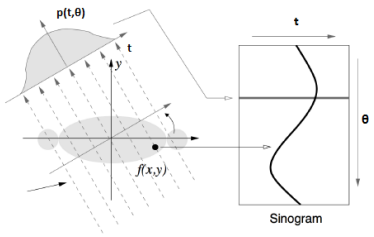

Figure 2.3: Sinogram, a representation in t,θ basis [15]

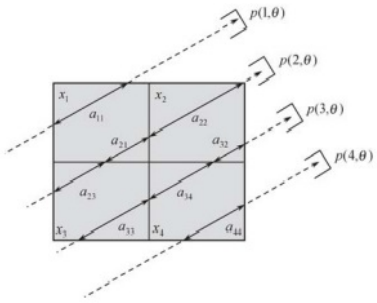

Figure 2.4: Discrete analog of the Radon Transform in a 2x2 matrix [15]

A quick demonstration of Radon Transformation can be performed in matlab using the radon function:

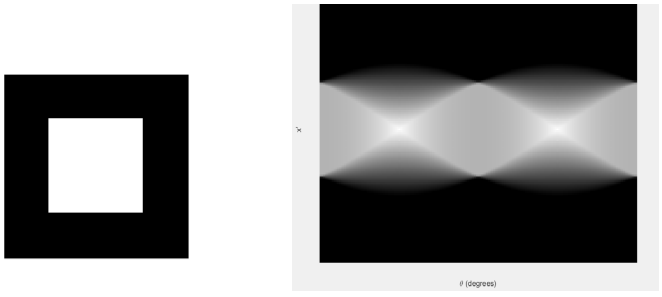

(a) (b)

Figure 2.5: a) Original Image b) Radon Transformation(sinogram) of the image [20]

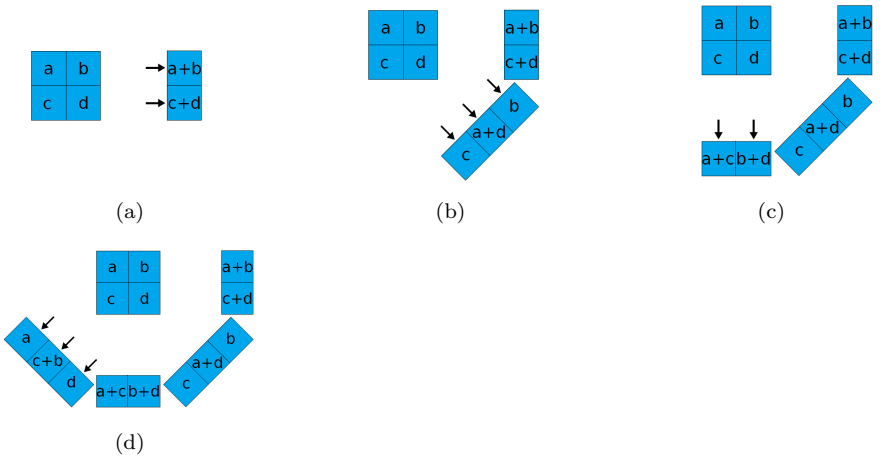

Figure 2.6: a),b),c),d): Illustration of the projection procedure. Each box represents a pixel and the letters a,b,c,d correspond to the intensity of each pixel. [15]

So far,everything that was mentioned is referred to data acquisition . At this point,there is a discrete intensity distribution coming from every captured angle. The target now is to obtain the original image from projections, only with knowledge provided by the sinogram.

2.3 Fourier Slice Theorem

Radon is linear. The Fourier slice theorem is the basis of tomographic image reconstruction. When a CT is performed, projections are measured. For every captured angle there is a set of line integrals for rays propagating in straight lines through the object.

Oftentimes a projection is called detector function. This function can be represented in Fourier space if a one-Dimensional Fourier transform is applied on it. So when projections are measured, there is a 2D representation of the object in Fourier space. Assume this representation is called $f(u, v)$. The target is to determine the original object $f(x, y)$. The estimate of the object $f(x, y)$ can be obtained if an inverse, two dimensional Fourier transform is applied. The Fourier slice theorem is the following statement: ***The one dimensional Fourier transform of a projection is equivalent to a two dimensional Fourier transform of a slice of the object f(x,y)*** Mathematically, this is expressed as follows:

$$f(u, v) = P_\theta(\omega) \tag{2.3.1}$$

,where $f(u, v)$ is the object function in Fourier domain and $P_\theta(\omega)$ the one dimensional Fourier transform of every projection.

Mathematical expressions for both $f(u,v)$ and $P_\theta(\omega)$ are the following:

$$f(u,v) = \int_{-\infty}^{+\infty}\int_{-\infty}^{+\infty} f(x,y)\cdot e^{-2\pi\iota(u\cdot x+v\cdot y)}\,dx\,dy \tag{2.3.2}$$

and

$$P_\theta(\omega) = \int_{-\infty}^{+\infty} P_\theta(t)\cdot e^{-2\pi\iota\omega t}\,dt \tag{2.3.3}$$

Proof: Start by substituting equation 2.2.1 into equation 2.3.3 and t will be replaced by the parameterization

$$x\cdot cos\theta + y\cdot sin\theta = t \tag{2.3.4}$$

$P_\theta(\omega)$ becomes

$$P_\theta(\omega) = \int_{-\infty}^{+\infty}\int_{-\infty}^{+\infty} f(x,y)\cdot e^{-2\pi\iota\omega(x\cdot cos\theta+y\cdot sin\theta)}\,dx\,dy \tag{2.3.5}$$

This equation will be identical with 2.3.2 if we change variables and assume that

$u = \omega\cdot cos\theta$ and $v = \omega\cdot sin\theta$

Substitution gives

$$P_\theta(\omega) = f(\omega cos\theta, \omega sin\theta) \tag{2.3.6}$$

, which is the desired result

Knowing the object function f(u,v) in Fourier space the original object f(x,y) can be estimated with an inverse Fourier transform:

$$f(x,y) = \int_{-\infty}^{+\infty}\int_{-\infty}^{+\infty} f(u,v)\cdot e^{2\pi\iota(u\cdot x+v\cdot y)}\,du\,dv \tag{2.3.7}$$

Although this mathematical model is not realistic : First, integral limits are infinite while there is a finite number of projections that are recorded,which leads to the previous discussion for the discrete Radon Transform in section 2.2.Also the function $f(u,v)$ in the Fourier space is known only at the points along the radial lines seen in figure 2.7, instead of square grids which are needed to perform the inverse Fast Fourier transform. Interpolation to the points in Fourier domain must be performed for the inverse transform. This procedure is more time- consuming to compile and more complicated. In the square grid case the Fast Fourier transform is applied to get the result. In the Fourier domain one can notice that the sampling distribution is dense in the origin , which means that low frequencies can be reconstructed precisely compared to high

frequencies, resulting to blurred CT's.In this way, important information from the sample is lost,because many useful details are included in high frequencies.

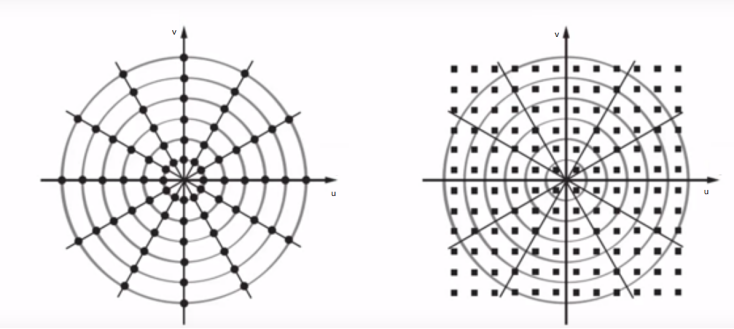

Figure 2.7: Fourier Domain. $f(u, v)$ and the square grid case with fast fourier transform [13]

2.4 Filtered Back Projection

During the projection recording step , in every angle the detector gets the total line integral of the object function. Now, in the back projection step, every point of the object will receive back the value from its detector function in that angle,meaning that every line of the sinogram returns to the object. The problem is that while re-distributing this activity back in the object, it is not known where intensity is higher or less,so equal activity is put for every ray path.Every point of the object which lies in a ray receives back the same intensity value.In fact,what happens is that the detector function or the line integral for an angle is smeared out in the object's domain.This process is repeated for all projection angles and the values are summed up.This procedure is called Back Projection.So with this process,the more the backprojected angles, the more the object will be distinguished.

It is known that in object's Fourier domain low frequencies are amplified, meaning that high frequencies that correspond to object's boundaries,details and sharp areas won't be distinguished.This will result again to a blurred reconstructed object.In order to get rid of this problem,a high pass filter is inserted to the reconstructed algorithm and multiplies with the detector function for every angle in object's fourier domain. With this filter lower frequencies become weaker and the object becomes clearer.The Fast Fourier Transform (FFT) is used for the detector function $P_\theta(t)$. The Fast Fourier Transform is an operation that converts a signal composed of N points in the time domain into N time domain signals of a single point .Next the N frequency components are calculated which correspond to the N time domain signals. There is an upper frequency limit in order to cut-off noise from high frequencies. Afterwards, the inverse Fourier Transform is applied and a new detector function is obtained.

This will be the function that gets back projected and gives the real object estimate $f(x, y)$.This process is called Filtered Back Projection (FBP).

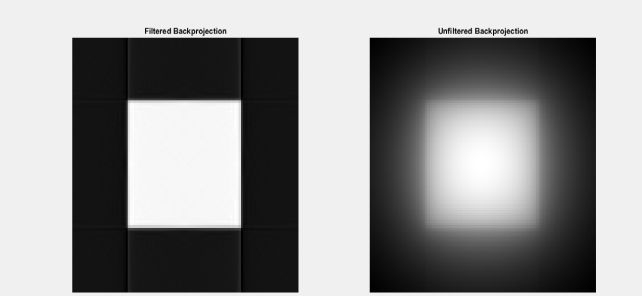

Figure 2.8: Back Projection vs Filtered Back Projection. Filtering clears the image [21]

A good illustration is a 2x2 matrix in figures 2.8 and 2.9 . Every matrix element represents a pixel and the values a,b,c,d correspond to pixel's intensity.

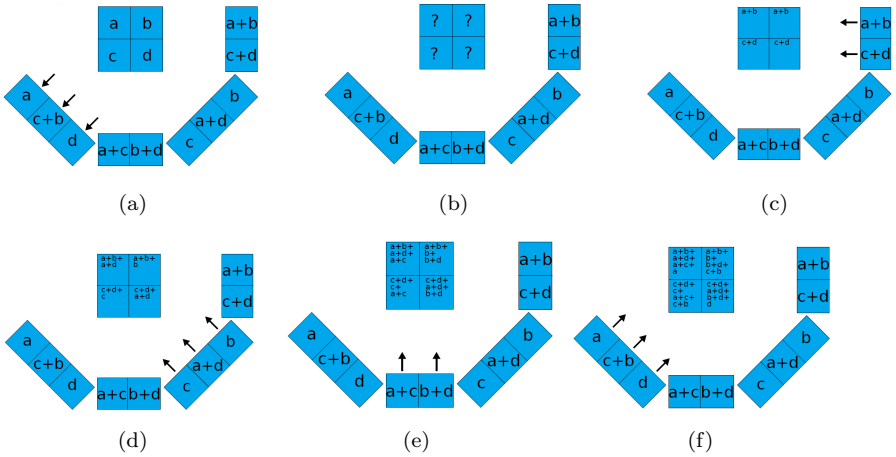

Figure 2.9: a)Projections, b)Back Projection, c),d),e),f): Smearing the projections back to the object

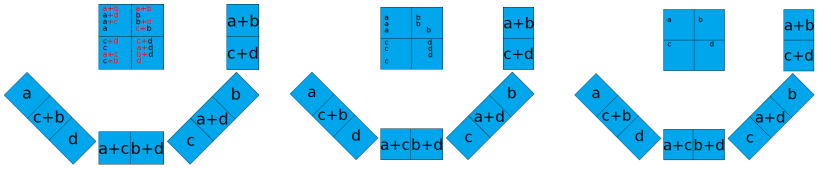

Figure 2.10: Continuing from figure 2.8 a): Projection intensity is subtracted from each pixel,b) Division with number of projections c)Original object

After the previous discussion the mathematics of back projection procedure can be introduced here .

It is known that the object $f(x, y)$ can be expressed as

$$f(x,y) = \int_{-\infty}^{+\infty}\int_{-\infty}^{+\infty} f(u,v)\cdot e^{2\pi\iota(u\cdot x+v\cdot y)}\,du\,dv \tag{2.4.1}$$

Switch to polar coordinates (ω,θ) from fourier basis (u, v): Make the substitutions $u = \omega cos\theta$ and $v = \omega sin\theta$. The differentials transform as $dudv = \omega d\omega d\theta$

we now get

$$f(x,y) = \int_{0}^{2\pi}\int_{-\infty}^{+\infty} f(\omega cos\theta, \omega sin\theta)\cdot e^{2\pi\iota\omega(x\cdot cos\theta+y\cdot sin\theta)}\omega\,d\omega\,d\theta \tag{2.4.2}$$

It is known that $x \cdot cos\theta + y \cdot sin\theta = t$ and from the Fourier slice theorem $f(\omega cos\theta, \omega sin\theta) = P_\theta(\omega)$, the integral becomes

$$f(x,y) = \int_{0}^{2\pi}\int_{-\infty}^{+\infty} P_\theta(\omega)\cdot e^{2\pi\iota\omega t}\omega\,d\omega\,d\theta = \int_{0}^{\pi}\int_{-\infty}^{+\infty} P_\theta(\omega)\cdot e^{2\pi\iota\omega t}|\omega|\,d\omega\,d\theta \tag{2.4.3}$$

This can be written as

$$f(x,y) = \int_{0}^{\pi} Q_\theta(x\cdot cos\theta + y\cdot sin\theta)d\theta \tag{2.4.4}$$

, Where

$$Q_\theta = \int_{-\infty}^{+\infty} P_\theta(\omega)|\omega| e^{2\pi\iota\omega t} d\omega \tag{2.4.5}$$

Now the function Q_θ is called the Filtered Back Projection with a filter of frequency response $|\omega|$. Contribution from filtered back projection to the reconstruction will be the same for all (x,y) points on the object that lie along every ray line L which correspond to a specific angle. Filtered back projection can be summed up in these 5 steps:

- Take the Fourier transform of all projections $P(\theta, t)$
- Multiply with the frequency filter
- Take the inverse Fourier transform
- Back Project all filtered projection
- Sum them for all possible angles

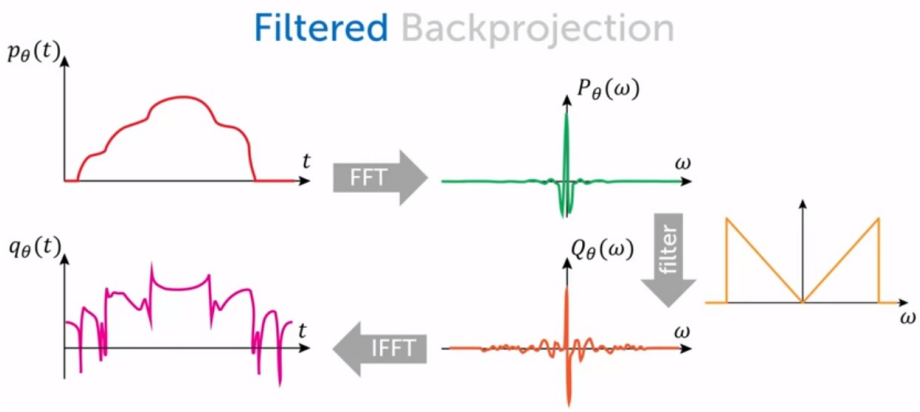

Figure 2.11: The Filtered Back Projection procedure [18]

2.5 3D Reconstruction

Previously the Fourier slice theorem was studied.This theorem states that the Fourier transform of a projection is equivalent with the Fourier transform of slice a of the object. If there is a large number of projections,the inverse transform can give a good estimate of the original object.Theoretically,if an infinite number of projections was available,the inverse fast fourier transform could give the exact estimate of the object.The Fourier slice theorem converts the process of measuring projections to estimate 2D slices of the object.

The mission for back projection is to place these values into the right place,their real origin.Then an estimate of the object can be obtained, by calculating the inverse fast Fourier transform and assuming that other projections do not contribute.The filtering process in back projection can be visualized as a weightening of each projection in the frequency domain. After performing back projection, the inverse Fourier transform is applied, and the weighted projections are summed up.After this procedure is applied, a stack with 2D slices of the object is obtained.If these slices are stacked together,the 3D Volume is built.

2.6 Image processing and Matlab code to produce 3D Volume

Tomography is a purely mathematical problem so an algorithm is required to build the 3D volume based only on projection data. Algorithm stages will be analyzed and explain every step that is done to obtain the volume.Image reconstruction is performed using Matlab. Raw data are edited with Imagej software. ImageJ is also used for the display of the 3D volume with the 3D Viewer function. When the filtered back projection procedure is done, a stack of 2D slices is obtained. If all these slices are stacked successively, the 3D Volume is obtained.

- **Algorithm Input**

The algorithm takes a .tif file as an input that includes projection data. Projection data are stored into a variable named NoP(=number of projections) in a matrix.

- **Raw Data Display**

Initially, the algorithm takes a .tif file where projection data is stored. Afterwards, a video is displayed with projection data to make sure the experiment gave the desired result and we can proceed further.

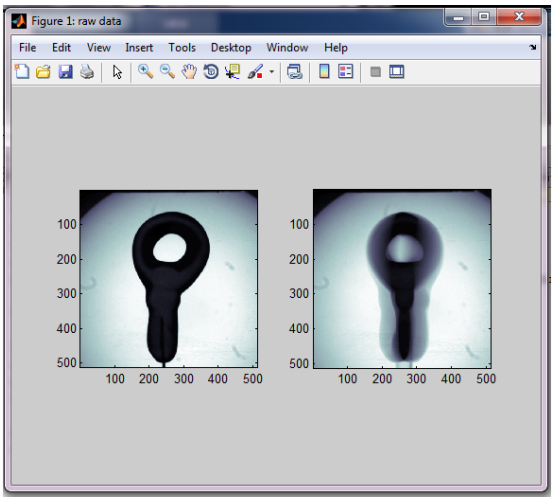

Figure 2.12: Raw Data

- **Offset Correction**

A reliable CT is obtained when axis of rotation is completely vertical to the camera axis and rotation axis is identical with the center of the image.The closer the axis to the image center, the better the quality for the 3D object.In this step, Matlab displays 2 projections:0˚ and 180˚. A cropping option appears in the graph.The desired area is chosen by creating a rectangle.It is recommended to choose an area(not the whole object) where the offset appears to be maximum.If not, select an area where the offset is desired to be minimized.

When rectangle of interest is chosen, matlab flips the ˚180 image and matches it with ˚0 projection.The algorithm moves both images from both left and right on the x axis and the opposite in order to find the point where offset is minimum. Obviously when two images are moved away from each other the offset increases and when they approach it decreases until minimum value is reached. In this way a graph is produced where a minimum value appears.This movement in x axis involves an area of about 100pixels for both right and left movements.Because of the camera that is used, offset appears slightly bigger. The reason for this is the 0˚ projection appears to be closer to the camera than the 180˚ projection.

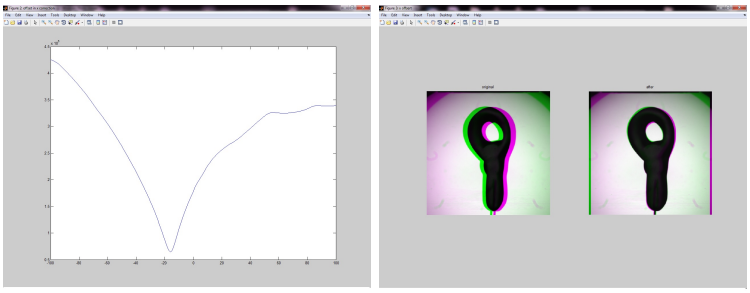

(a) (b)

Figure 2.13: Offset

- **Cropping the area of interest to be reconstructed**

Next step for the algorithm is to choose the area that will be reconstructed. The optimum choice is to select a small area where signal is more intense.This will also reduce algorithm's compiling time.Selected area is displayed next to the initial image.

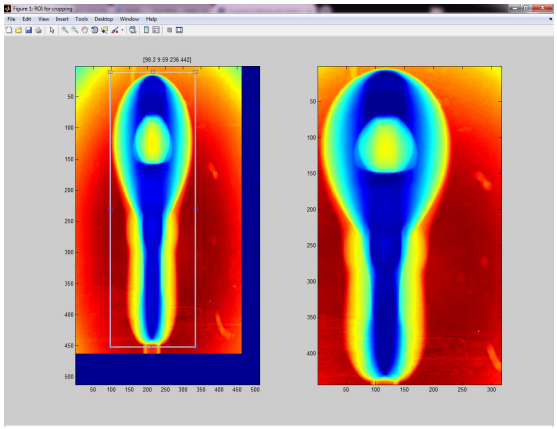

Figure 2.14: Cropping the area of interest

- **Sinogram**

The code displays the sinogram using matlab's radon function.

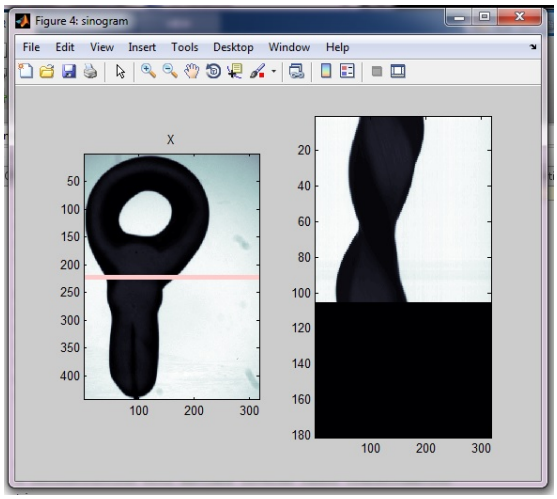

Figure 2.15:

- **Reconstruction filters**

At this point, the code displays a figure with the calculated sinogram and various reconstuctions performed with several different matlab filters used for the Back Projection step.

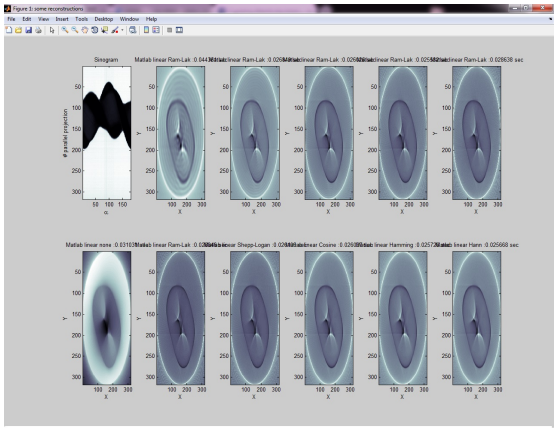

Figure 2.16:

- **Slice Viewer**

The 3D object is almost reconstructed. The code displays the performed reconstruction , where slices can be viewed from xy,xz and zy plane respectively.

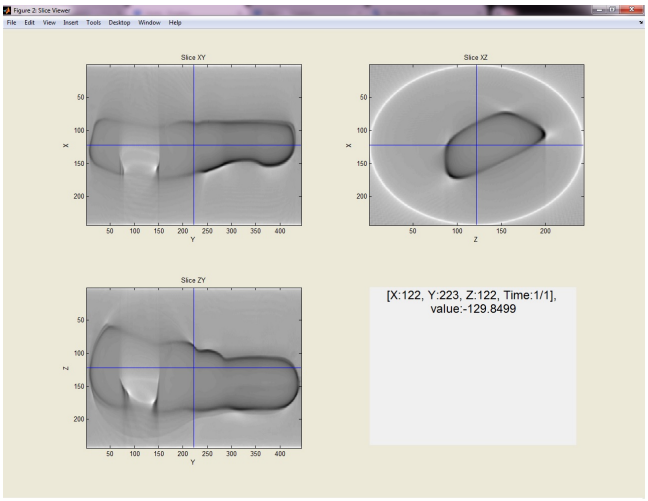

Figure 2.17:

When the tomographic reconstruction code ends, a stack with 2D Slices of the object is produced. With the help of ImageJ software and the 3D viewer function,these slices are stacked together and the 3D object is obtained

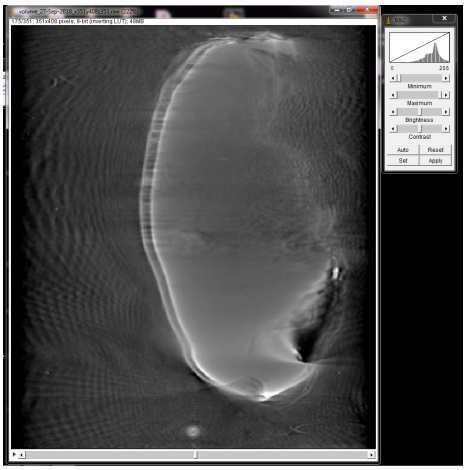

Figure 2.18: A .tif file that contains all 2D slices obtained from the reconstruction algorithm.The options next to the stack modify brightness/contrast in order for the volume to be clear and sharp.

Chapter 3

Experiments and results

3.1 Geometries used and working principle

3.1.1 OPT Geometries used

The experimental setup consists of 2 different used geometries:The first one is Transmission geometry and the second is reflection geometry. For the transmission case,a LED is used as an illumination source .The setup consists of a LED bulb, the sample, and a detector,a camera in this case. The amount of radiation that reaches the detector depends on the degree that it is absorbed by the sample, which is determined by the attenuation coefficient seen in chapter 1.Although this setup can give somehow decent or mediocre results, the reconstructed object will contain a lot of noise and the 3D result wont be what is expected. In order to obtain more specific information from the sample (considering also background noise in the experimental environment), 2 polarizers are interpolated in this setup.A polarizer transmits an electromagnetic wave where the electric field oscillates in one direction.Most of every day light is non-polarized,like light coming from the sun or a light bulb.This means that the electric field oscillates in various directions.The first polarizer will be placed right after the illuminating source to produce linearly polarized light in one direction.The other one is placed between the sample and the camera and can be either perpendicular or parallel to the polarization direction of the first one.The purpose of the perpendicular case is to record light coming only from the object.The reason that is detected is because light loses its initial polarization due to scattering from the object. Obviously, if there was nothing between the two polarizers, light would be blocked.The transmission geometry is used for absorption or scattering measurements .The second geometry that was used is reflection. Reflection is used for fluorescence measurements.For this purpose 2 different lasers are used.The lasers that were used were a 635nm He-Ne laser and an 514nm argon-ion laser.The reason why these two specific wavelengths were used will be explained later.

The following experimental analysis and applications will be performed using

a charge coupled device camera (CCD) which contains a sigma 50mm lens.The camera has 8 different diaphragms.Photography related concepts will be analyzed subsequently. For the Transmission case,as an illumination source a white light LED bulb is used combined with a diffuser , in order to get a homogeneous beam to strike the sample.The LED has a power supply that allows to change the intensity.This gives the ability to avoid saturation effects on the camera. Experimental setup will be such that the sample is loaded from above, using a rotation stage as seen in figures 3.3 and 3.5. The whole process of reconstruction is done in 2 big steps.The first one is purely experimental and linked with data acquisition.Data acquisition is done in Labview environment.The are a number of things that need to be checked in order to get a reliable optical CT.Before any experiment, always make sure that the center of the image is identical with rotation axis .In this way lots of artifacts will be avoided .The second step is the use of a reconstruction algorithm based on the acquired projections to build the 3D volume .The algorithm is designed and compiled in matlab,as it was analysed in section 2.6.

(a)

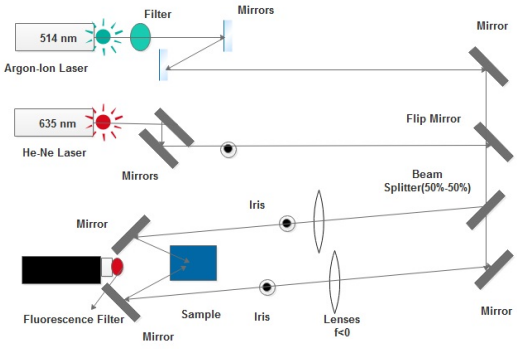

(b)

Figure 3.1: OPT geometries used for a)Transmission and b) Reflection

3.1.2 Fluorescence

A big part of the experiments will be linked with Fluorescence, a natural phenomenon that needs to be further studied. Fluorescence is the emission of light from a molecular substance(organic or not) immediately after it is radiated from another light source. When a substance is irradiated with light, the photons of energy $h \cdot f$ are absorbed by the substance.When these photons are absorbed, they excite substance's electrons to higher electronic states. Electrons return back to their ground state emitting light .The substance absorbs a part from the incident energy and radiates light of lower energy due to conservation of energy, which corresponds to larger wavelengths.For example, when a dye is irradiated with UV radiation,it is expected to emit light in the visible region of the EM spectrum. Light absorption and radiation are also known as absorption and emission respectively.

Due to evolution of microscopy techniques through the years, fluorescence phenomena could be studied more frequently by biology and material sciences in order to explain several biological mechanisms and determine the properties of various materials. Now every dye has an excitation and emission spectrum. This spectrum is obviously continuous. Each of these curves have a maximum intensity value. At this particular wavelength that corresponds to this maximum, fluorescence phenomenon is very intense.The spectral distribution of emitted light from a dye does not depend on the radiation source. Also, excitation and emission curves can be different when the environment of the dye is changed. For instance, pH and dye concentration can result to new , shifted excitation and emission curves. [35]

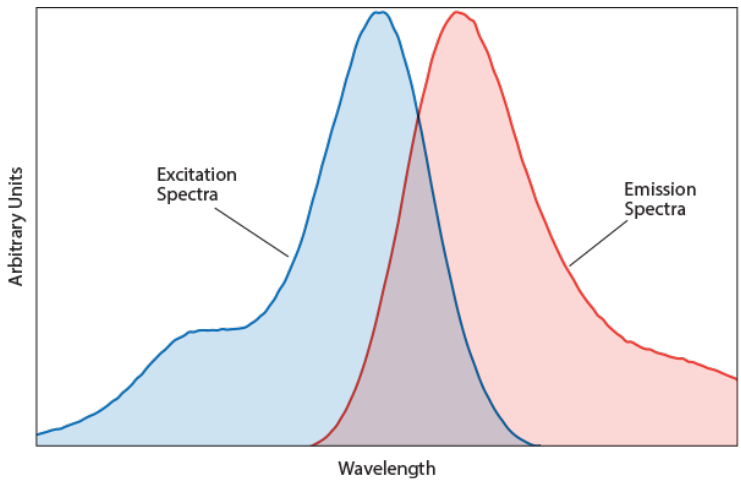

Figure 3.2: Fluorescence spectrum.Blue curve corresponds to excitation spectrum and red curve to the emission curve. Notice emission spectrum is in a larger wavelength region. [35]

Another way to visualize this type of processes is the Jablonski Diagram. A Jablonski diagram is an energy diagram. On the vertical axis is energy with every column representing a specific spin multiplicity.Bold columns correspond to the limits of electronic states.Within each column horizontal lines are the eigenstates for that molecule.For every electronic state there are multiple vibronic states. These vibronic levels can be divided into rotational states.Usually these details are not shown in the diagram.In figure 3.3 , there are 4 possible processes : Absorbance,Vibrational Relaxation and Internal Conversion , Fluorescence and Intersystem crossing.

Absorbance is the process of exciting an electron from a lower energy level to a higher one.In order for absorbance to occur in a molecule, light wavelengths used must be equal to the energy difference between two eigenstates of the molecule. Absorbance is a very fast process and times intervals are on the order of $10^{-15}s$, indicated with a purple arrow in figure 3.3.

When an electron is excited, this energy can be transferred in more than one way.One way is through Vibrational Relaxation, where the energy provided by a photon to an electron is given to other vibrational modes as kinetic energy. This energy could remain to that molecule or it could be transferred to other molecules around the excited one.

Internal conversion occurs when vibration levels strongly overlap the electronic ones.As a result, the excited electron can transfer from a vibrational level in one electronic state to another vibration level in a lower electronic state.These two processes are indicated with a green arrow in figure 3.3.Fluorescence is also shown with an orange arrow in figure 3.3.

Intersystem Crossing is another process in a Jablonski diagram.In this case the excited electron changes spin multiplicity from singlet to triplet.It is the slowest process in a jablonski diagram.Although this transition is forbidden by selection rules,if coupling vibrational factors are considered,the transition becomes weakly allowed.The return to ground state could happen either with phosphorescence, a radiative transition from excited triplet state to singlet ground state or with delayed fluorescence, the transition to the first excited singlet level,that leads to transition to the ground electronic state for emission.

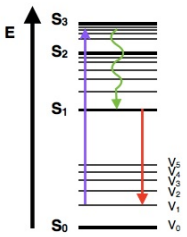

(a)

Transition	Time Scale	Radiative Process?
Internal Conversion	10^{-14} - 10^{-11} s	no
Vibrational Relaxation	10^{-14} - 10^{-11} s	no
Absorption	10^{-15} s	yes
Phosphorescence	10^{-4} - 10^{-1} s	yes
Intersystem Crossing	10^{-8} - 10^{-3} s	no
Fluorescence	10^{-9} - 10^{-7} s	yes

(b)

Figure 3.3: a)Jablonski Diagram,the processes are: Absorption(purple arrow),Vibrational Relaxation(blue arrow),internal conversion(green arrow), b) Table with timescales for radiative and non-radiative processes [22]

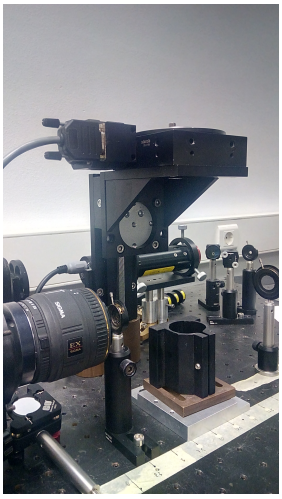

Figure 3.4: Setup to load the sample.

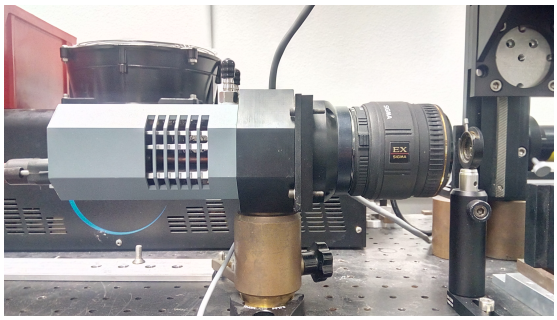

Figure 3.5: Camera used to record projections.

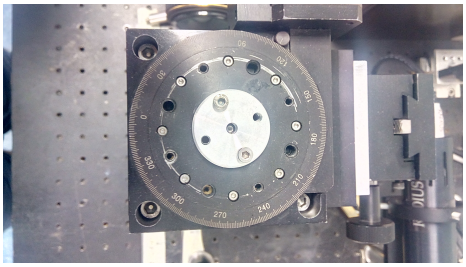

Figure 3.6: Stage used to rotate the sample

3.2 Photography concepts and experiment

A first and crucial step before starting the experiments is to get a good understanding of the camera and how to handle the sample.Depending on sampe's dimensions, the right sample-camera distance needs to be determined .Camera can be thermoelectrically cooled down until almost -50 °C. This feature can reduce camera noise during experiments and decrease image capturing exposure time as well.

Before proceeding with the reconstruction step, it must be confirmed that system parameters are optimized and produced the best data quality as possible. If this step is failed, reconstruction will be poor and full of artifacts. Some photography concepts will be introduced here.These concepts will optimize the step of capturing projections.Before the volume of the sample is build , projections must be clear and detailed.For instance,the whole sample must to be in focus .The following parameters can be modified to improve data quality: Diaphragm,Field of view,Depth of field,Camera Exposure Time.These concepts will be explained with details.

3.2.1 Diaphragm

A diaphragm is an aperture with varying diameter.This aperture controls the amount and intensity of the light that makes it to the camera sensor. In most cases,when dealing with diaphragms,this is the notation seen in the lens:

Figure 3.7: Diaphragm values in a camera

As seen in figure 3.8, there are some values, but what do they stand for? We could say that they are the diameters of the aperture but that is not completely true. In fact, these values correspond to lens focal length divided by aperture diameters. Ultimately, the smallest value, 2.8 in this case, is the value that leaves most of the light to make it to the camera sensor.Similarly, the highest value (32) blocks most of the light.So with the use of diaphragms illumination of the object can be modified without changing the source. In the image below the effect of the diaphragm is seen while capturing images at different values:

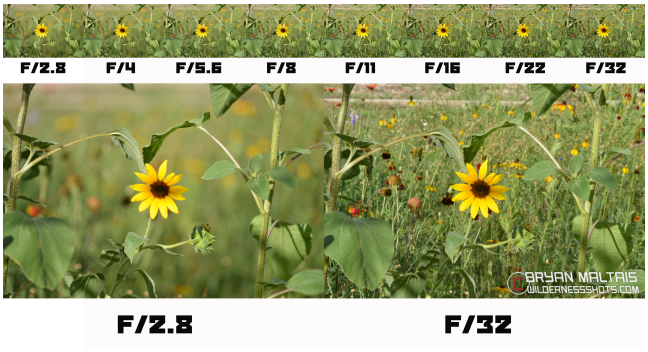

Figure 3.8: Effect of Diaphragm in capturing images [25]

Figure 3.9: Aperture diameter for different diaphragm values [25]

3.2.2 Optical Surface

Optical Surface or Field of view is another important parameter while measuring an object with optical CT.Optical Surface is the observable area from the camera. Camera's lens has a specific focal length, but when camera-sample distance is changed,the field of view is also going to change. In general, while working with a camera,there are 3 different ways to modify field of view: 1) Replace the camera lens with one of different focal length, 2) Change the distance of the object from the camera and 3)use another camera . For practical purposes, in our experiments we are going to change the camera-object distance.

Sample-camera distance will be modified to understand what are the limits for the dimensions of samples in order to fit the available field of view(smallest and biggest) .This variation in sample-camera distance will make the sample appear out of focus.For example a large aperture can cause this effect. When the sample is out of focus,it's details wont be sharp focus and the background stuff will look blurred. On the opposite, if a small aperture is used, a larger part of every projection will be in focus.

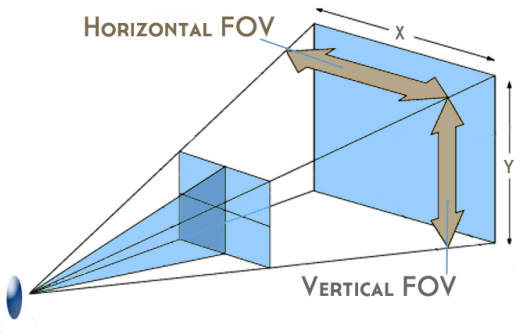

Figure 3.10: Illustration for Optical Surface/field of view [23]

3.2.3 Depth of field

Depth of field is the maximum distance in which the sample appears to be in focus . Depth of field is determined by the diaphragm value that is used. The lowest value of the diaphragm aperture corresponds to the minimum depth of

field and vice versa for the highest value.So the whole sample will appear clear and in focus . In general, depth of field is associated with image resolution.

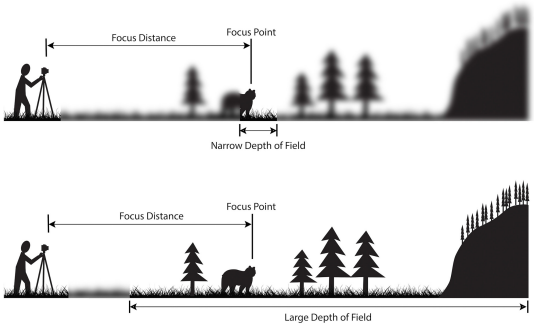

Figure 3.11: The Concept depth of field [27]

Depth of field is affected by:

- **Aperture** , because large apertures (which correspond to small values in camera) produce very narrow depth of field .The opposite happens with small apertures(large numbers in camera).
- **Camera-object distance**. When this distance is small, depth of field also decreases
- **Focal Length of the lens**. Small lens focal lengths produce bigger depth of a field than the ones with long focal length
- **Size of the used sensor**. When cameras with small sensors are used depth of field increases.

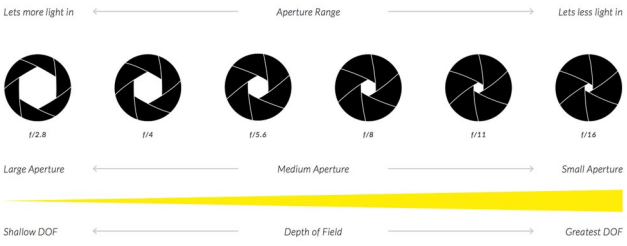

Figure 3.12: Aperture and depth of field relation [26]

3.2.4 Camera Exposure Time

Exposure time is the time interval the sensor is receiving signal from the light source .Camera Exposure time is another way to control the amount and intensity of light that reaches the detector. It is suitable if saturation effects (high intensity values) must be avoided.

3.2.5 Dimensions of OPT samples

It is important to know what dimensions should the measured object have in order to measure it with the OPT setup. Before starting the experiments,it is recommended to know in which distance the sample should be placed from the camera. This will make the sample appear in focus and inside depth of field. The purpose is to optimize everything in order to get a reliable optical CT.The following procedure is used to estimate the dimensions of samples that can be used.For this purpose a piece of millimeter paper is attached in a screen.

For different screen-camera distances, the screen is focused and field of view is measured. This procedure is done for 2.8 and 4 diaphragm. We notice that linear fit for both diaphragms is almost the same, slightly changed.This is something that is expected, because in field of view the only concern is camera's observable area.From these to graphs,it can be seen that the limits for field of view are an 3cm$x$3cm optical surface and an 9cm$x$9cm optical surface.This means that sample dimensions must be such that they could fit in these optical surfaces, in order to be measured.

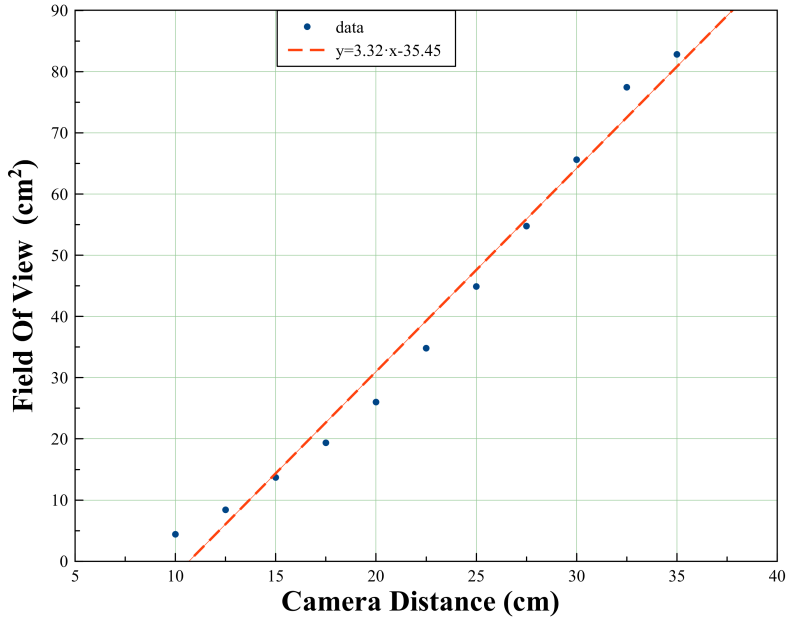

Figure 3.13: Optical surface estimation for 2.8 diaphragm.

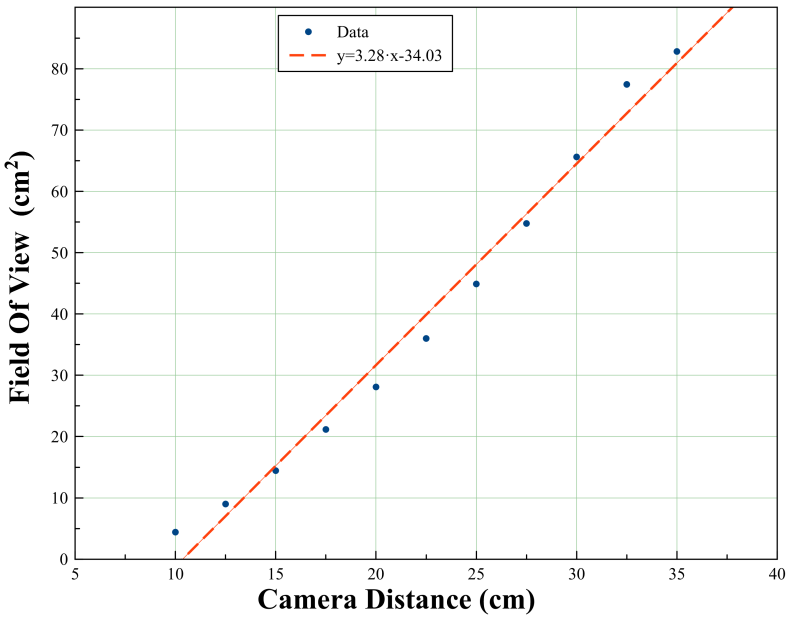

Figure 3.14: Optical surface for 4 diaphragm.

3.3 Experiment Preparation and recording Projections

3.3.1 Experimental Parameters

The whole process of data acquisition will take place in Labview environment. Before examining software's details a list will represent all parameters that can be controlled in the experiment:

- **All camera parameters** that were mentioned before. Every time a sample is about to be measured, the following procedure needs to be done: We need to focus on our sample and make sure that all of it is inside the depth of field area. For this purpose, the widest of the diaphragms (smallest value in the camera , in our case 2.8) is used and then attempt to focus on the object . In this position there is the narrowest depth of field. The experiment is now ready to get going.
- **Polarization type** If we use the transmission geometry,the 2 polarizers can be vertical-parallel or parallel-parallel. vertical-parallel measures scattering and parallel-parallel measures absorption.
- **Camera Thermoelectrical cool down** Camera can be thermoelectrically cooled down and control this process with labview. This procedure will take a few minutes before it's ready.

- **Acquisition Step** Depending on the precision needed, a big or very small acquisition step can be chosen. In most of the cases 1 or 2 degrees will be used as acquisition step. The smaller the recording step, the more projections so the Filtered Back Projection algorithm gives a better estimation of the object.
- **Camera Exposure Time** This is another way to control the amount and intensity of light illuminating the sample.

3.3.2 Labview Environment

When labview is launched, the software asks for input the equipment used to run the experiments.When the experiment is done, a .tif file is produced with projection data.

Firstly, the software is open ,as seen in figure 3.12 . A window opens showing two images, one shows the white light image and the other one shows the background image. On top of the window there a series of options. Before starting the experiment, background and white light images are captured. White light image is just a picture of the surface of the sample, with illumination from camera side. By clicking Camera $\longrightarrow$ Measure Backround and White light $\longrightarrow$ these images are captured. The program also allows to move the stage , for example motion on x and y axis and make a specific rotation angle. Next, to thermoelectrically cool down the camera we choose camera $\longrightarrow$ Change Temperature.

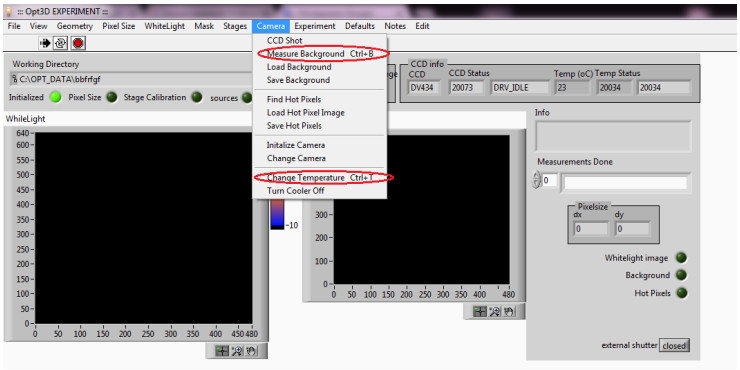

Figure 3.15: Labview environment.White light- Background Image and thermoelectrical cool down for the camera

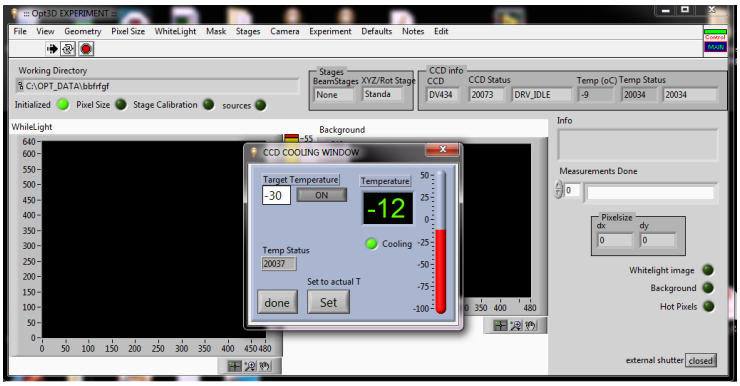

Figure 3.16: Camera thermoelectrical cool down procedure

To modify temperature, camera⟶ Change Temperature option is selected.A new window opens as seen in figure 3.11. Target temperature is chosen and then the "go to temp" option is selected. This will take a few minutes until target temperature is reached. When cooling procedure ends we click "done".

Before starting the experiment,the sample must be focused on and confirm that the whole sample is inside depth of field. This can be done by choosing Camera ⟶ CCD shot. This function allows to take as many images as wanted with the option to save them. Sometimes it's more suitable to take automatically capture several projections of the sample by choosing the "repeat" option.This option is very useful while trying to detect parallel and perpendicular polarization.

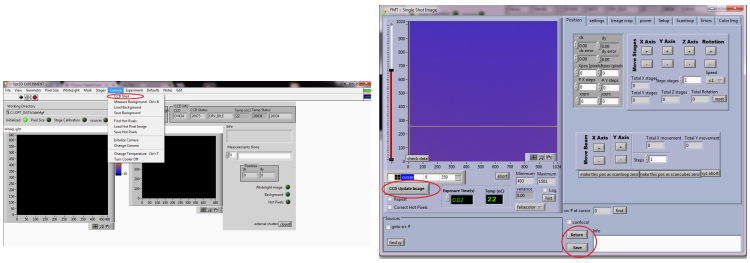

(a) (b)

Figure 3.17: Experimental Setup: (a)Choosing single shot option, b)Single shot environment. The "repeat" option keeps getting constantly photos of the object with period equal to camera's exposure time.

Figure 3.18: Running the experiment

When temperature is ready, we proceed to the experiment. The option Experiment $\longrightarrow$ Run experiment is selected. A new window will open and experimental parameters have to be chosen. These parameters are saved in a .txt file that will appear along with with projection data in the chosen working directory . This .txt file records the light source, type of polarization, diaphragm chosen,acquisition step and possible filters used, and any other details that we put into it. "Run experiment" option is then selected to start the experiment. A new window opens which shows how many projections are captured, every projection captured, and next to it the overall result.Overall result means the summed intensity from all projections.This is the procedure for every measurement. When the whole procedure ends , the .tif file is opened with imageJ software to check projection raw data. ImageJ is an image processing software .More functions of this software will be analyzed next.

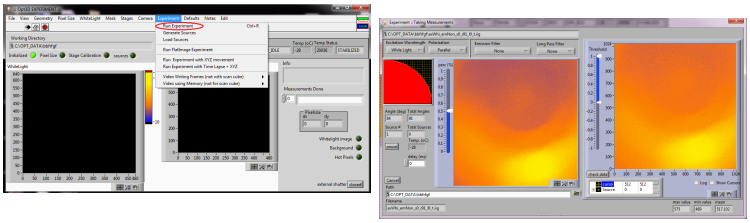

(a) (b)

Figure 3.19: a) b) Running the experiment

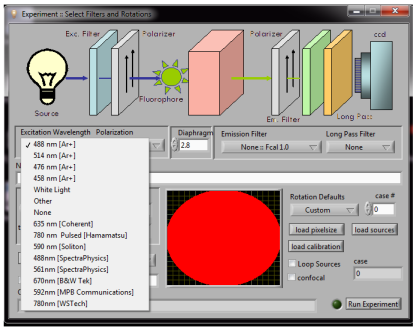

Figure 3.20: Choosing parameters used for the experiment.This information is saved in a .txt file

3.4 Loading the sample

Up until now the whole experimental procedure is completely analyzed.The sample that will get an optical CT was chosen .How are we going to load the sample? This is a complicated problem that largely depends on the type of sample. In this case, the sample that will be loaded in O.P.T is the skull of a mouse.This problem is in fact split in two: 1) The first one is how are we going to load the skull without causing any damage to it, and make more than one experiment and 2) What base should be constructed for the sample?

After some testing, the skull will be embedded inside an 1% agarose gel.Agarose is a polysaccharide that is extracted from seaweed. It's gelling temperature is between 30°-50°C with melting temperature 90°-95°C,close to water's boiling temperature. The skull with the agarose gel are kept inside a syrigne in order for the gel to obtain a cylindrical shape. In this way the gel could be placed to the rotational axis as it can be seen in figure 3.21. Now, for base,it will be a metal disc with four flanges , all together attached to a post (figure 3.20). The specimen is held by inserting needles through the agarose gel. The needles are inserted through the flanges which contain pre-drilled holes.

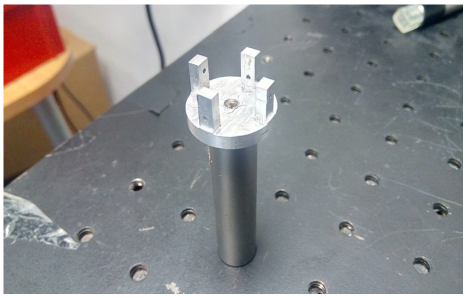

(a)

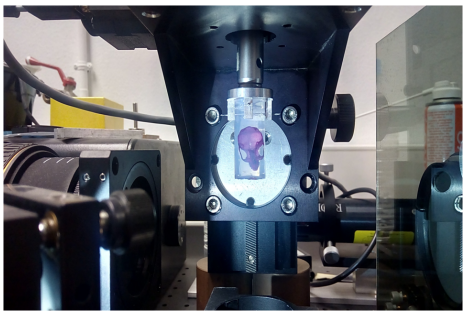

(b)

Figure 3.21: a)Constructed base to load the sample. Each flange has a drilled hole to insert the needles and load the sample,b)Skull inside 1% agarose gel

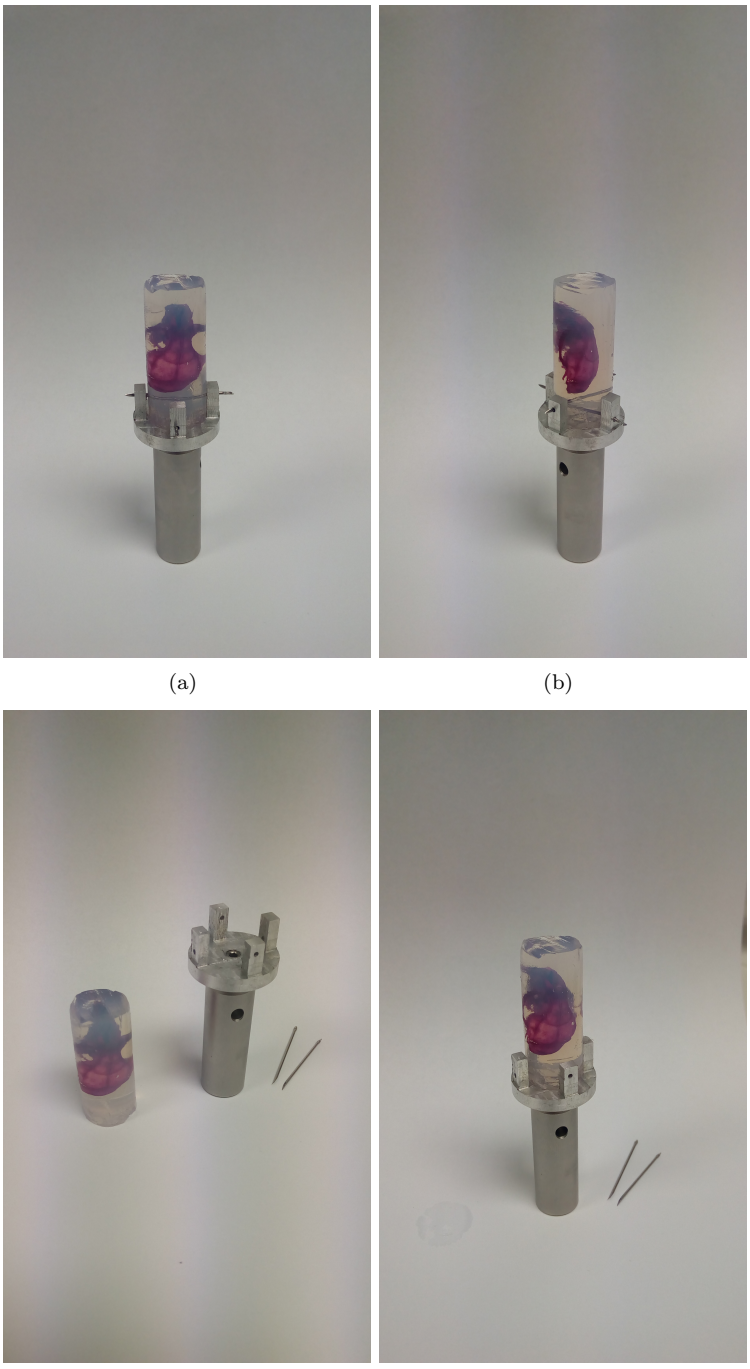

(a) (b)

(c) (d)

Figure 3.22: a),b),c),d) Loading the sample using needles and the constructed base

3.5 Transmission Measurements

A first test for the 3D volume reconstruction algorithm will be performed on gummy bears. The reason gummy bears are chosen as a first test is because they are transparent enough and can be handled quite easily , so they seem ideal for some quick testing. The sample will be loaded from above with the setup analyzed in section 3.1 .It is excepted from the parallel case to measure absorption,meaning that camera the records the remaining signal after it is absorbed by the sample.In the parallel case, signal is more intense outside the sample The perpendicular case corresponds to scattering, the signal coming only from the object is measured. Now signal coming from the sample is more intense than outside.

Figure 3.23: Projection data from imageJ in 512x512 binning with 1° step.

Reconstruction algorithm was used to produse the volumes for parallel and perpendicular polarization.These are the resulted objects:

(a)

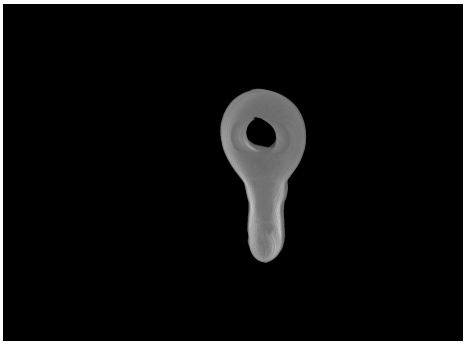

(b)

Figure 3.24: a)Raw Data for Parallel Polarization b)3D Volume Projection

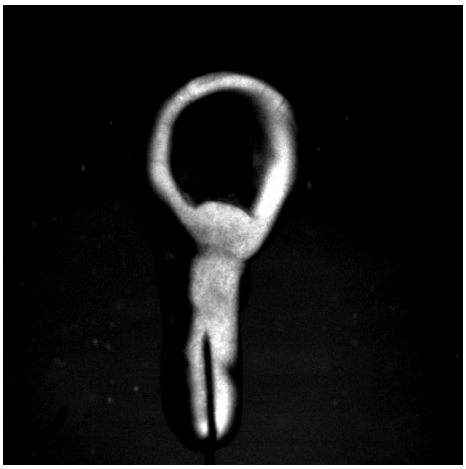

(a)

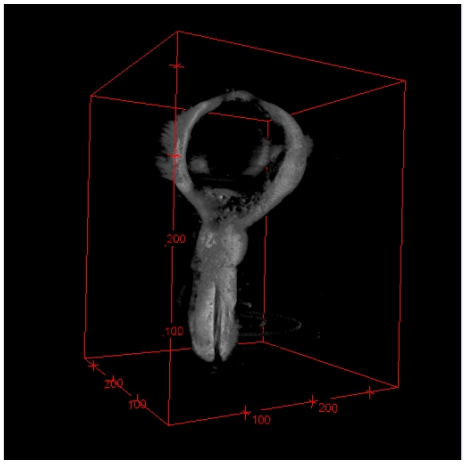

(b)

Figure 3.25: a)Projection Raw Data for Perpendicular Polarization b)3D Volume

3.6 Measuring the dimensions of an object

In this section the dimensions of an object will be measured experimentally.Firstly, we start by calculating pixel size. In order to calculate pixel size, a piece of millimeter paper was attached in a screen.Every "box" in this paper is separated every 1cm. So, if the distance is measured in pixels, pixel size can be obtained. For this purpose ImageJ is used. We find that 1 pixel corresponds to 45 microns. The object that was used is almost transparent. All projections are captured with the OPT setup using the Transmission geometry. Used acquisition step

was 2 degrees,meaning 180 projections were captured.Matlab is used to produce the 3D Volume. The experiment is repeated for different acquisition steps: 3,2,1 and 0.8 degrees respectively. As expected, the less the angular step the better the optical CT in terms of details and sharpness.The more projections are acquired,the better results are obtained when applying the filtered back projection algorithm.

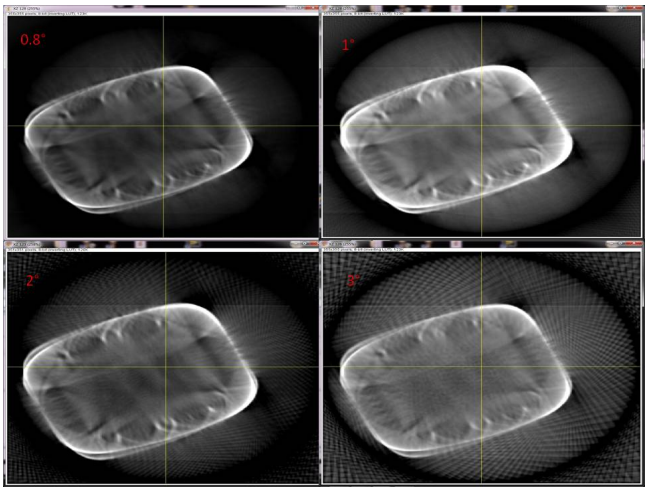

Figure 3.26: Projection data Comparison using ImageJ for XZ slices

Both vertical and horizontal dimensions of the object will be measured. Again,ImageJ is used for the analysis. We are going to experimentally measure every dimension by analyzing the signal that makes it to the camera. For this purpose, parallel polarization case will be preferred . The reason is signal is more intense outside the object, so the 2 points where the intensity drops are identified.These 2 points are the boundaries of the object. This area corresponds to absorption from the sample. This distance is measured in pixels and then the calculated pixel size is used (1pixel$\rightarrow$45μm) to convert this distance in mm and get the experimental value. For measurements, ImageJ option Image$\rightarrow$Stacks$\rightarrow$Orthogonal Views was used.

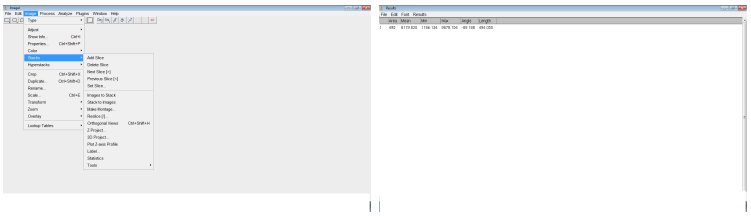

(a) (b)

Figure 3.27: a) and b) Measuring process using ImageJ

Measuring results are represented in the following table. **The original dimensions of the object are 11.00 and 8.70 mm respectively:**

Angular step(deg)	**Dimension 1(mm)**	**Dimension 2(mm)**
3	10.53 ± 0.08	8.29 ± 0.06
2	10.55 ± 0.05	8.3 ± 0.1
1	10.56 ± 0.04	8.2 ± 0.1
0.8	10.50 ± 0.04	8.3 ± 0.1

3.7 Imaging the skull of a mouse with Transmission geometry

The Transmission OPT setup as it was described in section 3.1 will be used to image the skull.It's diameter is approximately 15mm, making it suitable for OPT measurements. LED's intensity can be modified, also the lamp has an attached diffuser .One can easily wonder why agarose is used? The reason is that agarose is a gel that is pretty close to a water solution. Also, agarose is transparent and does not interact with the skull or it's dyes. Although agarose itself won't be enough to produce a good looking optical CT. A major drawback while measuring the sample in the gel is this: While analyzing raw data there is dust in the surroundings of the gel. Also there are refraction effects in the gel because it's refractive index is slightly bigger than air.In order to solve this problem, the agarose gel is loaded inside a water bath. This improves raw data quality for further analysis.In transmission geometry, the absorption of the sample is measured. So the 3D object is basically a mapping of the attenuation distribution of the sample.From figure 3.28 one can observe what was mentioned in section 3.1 :The parallel case measures absorption and the perpendicular case measures scattering,because camera records signal coming from the skull.

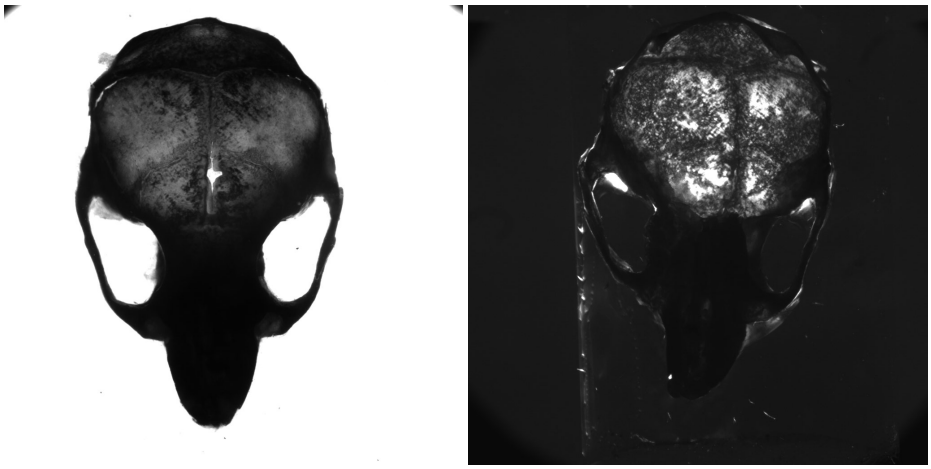

(a) (b)

Figure 3.28: Projection data for a) Parallel Polarization b) Perpendicular Polarization

3.8 Fluorescence measurements

3.8.1 Fluorescence and dyes of the skull

The next step after measurements with the Transmission setup using the LED as illumination source is to replace the LED with a laser in the experimental setup. The reason these two wavelengths are chosen in the reflection geometry is to observe fluorescence from the two dyes that the skull is painted.These two dyes are Alizarin Red S and Alcian Blue. A laser can still give good quality results because it is another form of visible light, although now fluorescence will be measured.In order to be able to measure with a laser as light source, a way must be found to expand the beam.Beam's diameter must be at least the same with skull diameter(15mm) to cover the whole specimen homogeneously. This is a bit different from the OPT principle that has been seen seen so far where signal is affected by either absorption or scattering. This signal now will be coming from the sample itself and illumination source will be used to excite the dyes the sample is painted with. More information will be provided about the dyes below:

- **Alizarin Red S**

Alizarin Red S is a dye that is insoluble in water, moderately soluble in ethanon,toluene,xylene and pyridine acid. Also it is freely soluble in hot methanol. Alizarin's melting point is found at 290°C and it's boiling point is found at 430°C. Alizarin's pH range is between 5.5-6.8 and 10.1-12.1. This dye is used in solar cells,plasma

display panels, antireflective coatings, chemical mechanical polishing and various other applicaitons. In the following figures absorption and emission curves are observed for the alizarin dye :

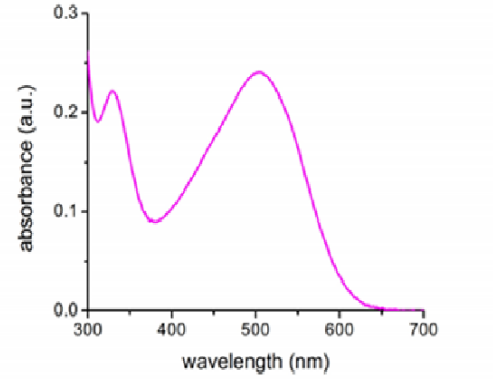

(a)

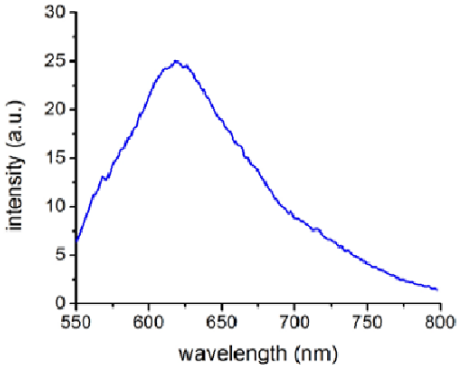

(b)

Figure 3.29: a) Alizarin's absorption spectrum b) Alizarin's emission spectrum [37], [44]

The environment and solution where the dye is placed affect the emission spectrum. It is known for alizarin that emits in the range 575-675 nm .

- **Alcian Blue**

Alcian Blue is a dye that is soluble in water and in ethanol. It's melting point is found to be at 148°C. This dye is used in various biological applications and for industrial stuff like inks.In figure 3.31 there is alcian's absorption spectrum . Alcian Blue emission spectrum has a maximum at 674-682 nm.

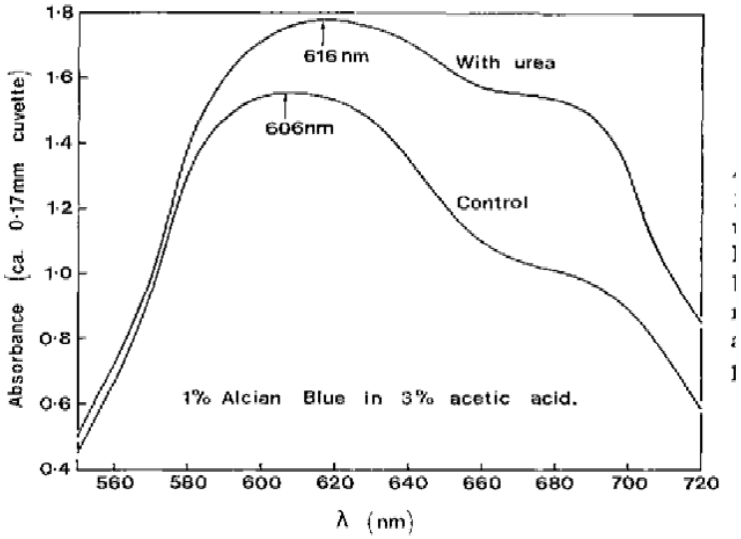

Figure 3.30: Alcian's absorption spectrum in 2 different solutions. [39], [40]

The spectral characteristics of these 2 dyes are represented on the following table. The notation used on the Filter used column is **filter's central wavelength/bandwidth** and it's about the filters attached to the camera in order to obtain signal from each dye, using the 2 lasers shown in the reflection geometry

Dye	Excitation	Emission	Filter used 0
Alizarin Red S	514nm	575-675nm	615nm/90nm
Alcian Blue	635nm	674-682nm(max)	700nm/75nm

3.8.2 Transmission Geometry using lasers

The spectral characteristics of the dyes the skull is painted are known. Based on this analysis, the transmission geometry is used to measure the skull. Initially, the 635nm He-Ne laser was used. The target was to guide the beam with mirrors, using iris to filter the beam. Also, a telescope was used. The telescope consisted of 2 converging lenses, where the second focal point of the first lens is identical with the first focal point of the second lens. This is called 4f telescope.The purpose of using the telescope was to expand the beam to illuminate the whole sample while the beam remained parallel.

This setup could not give the desired result because the quality of the beam was bad.Another idea was to use a pinhole($100\mu m$ diameter) to achieve a large and homogeneous enough beam diameter.This setup could not produce a clear 3D object because the recorded signal is weak due to the pinhole used.In general, while working with transmission geometry using a laser to observe fluorescence, there is absorption from the sample, so the signal detected from fluorescence is

weak.The final idea to expand the beam was the use of a lens of negative focal length in transmission mode. Experiments showed that negative lenses along with the use of iris could produce good projection data, so they were used for the reflection geometry.

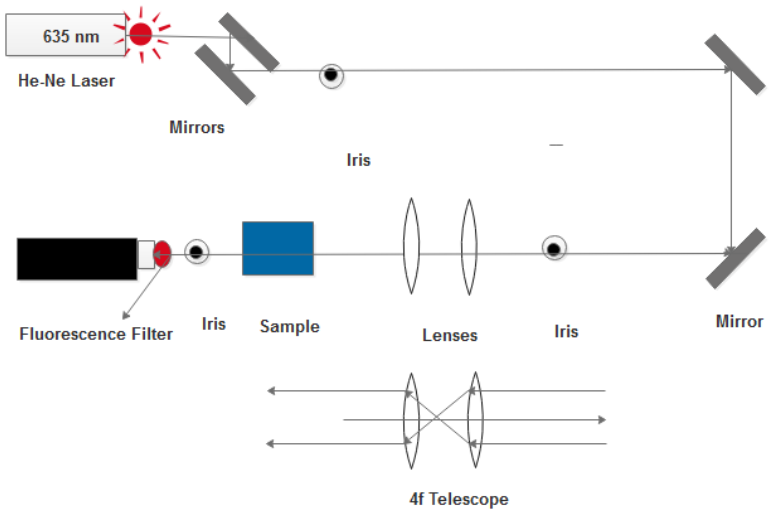

Figure 3.31: First setup.Beam quality was poor. [45]

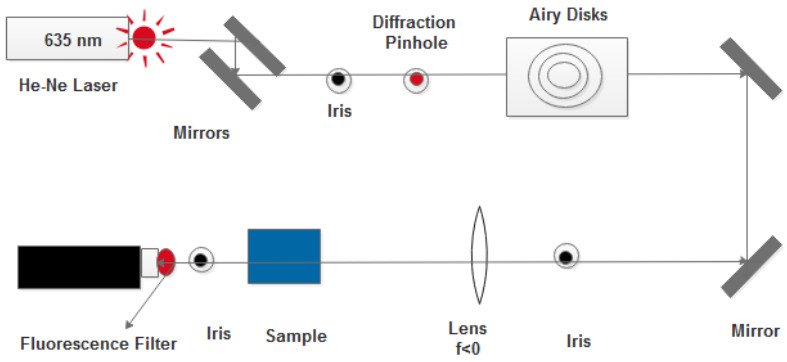

Figure 3.32: Second attempt.Signal that reaches the camera is very weak because of the pinhole used. [45]

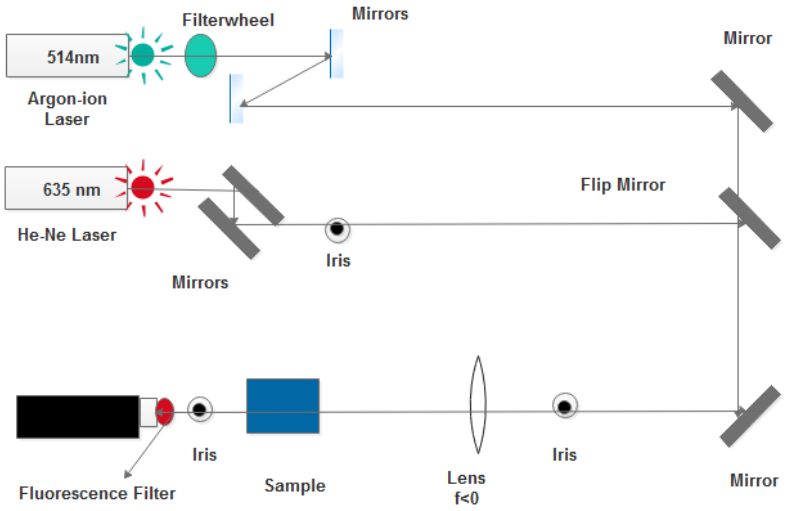

Figure 3.33: Final setup for transmission .The negative lens was used for the reflection measurements,transmission's signal was weak. [45]

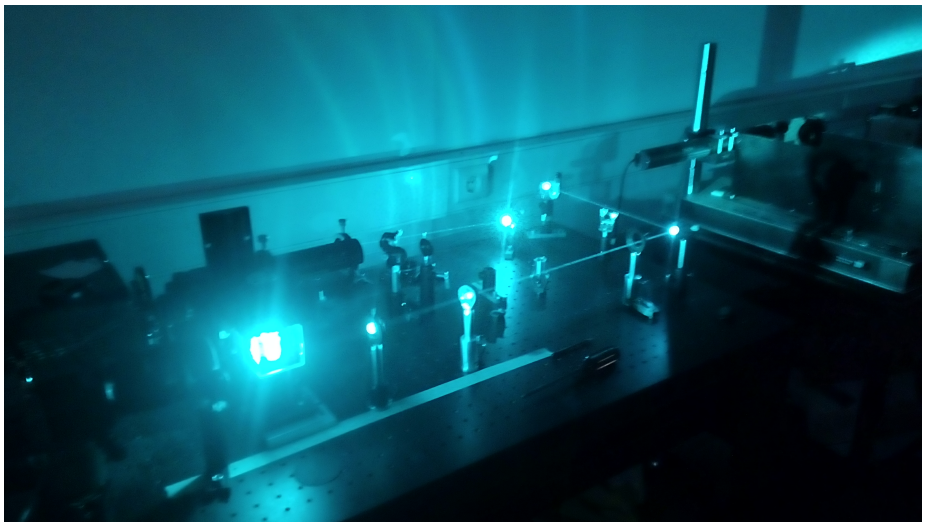

Figure 3.34: Argon-Ion Laser operating in high intensity in transmission geometry

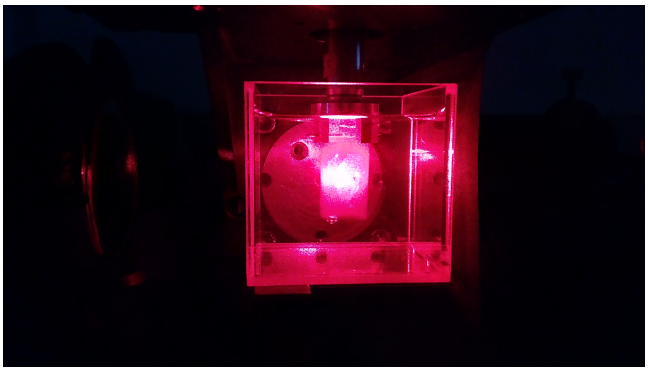

Figure 3.35: Specimen Illumination with He-Ne Laser in transmission geometry

3.9 Skull Fluorescence with reflection geometry

For the reflection geometry, the setup shown in figure 3.37 was used.The beam for each laser used is guided with mirrors to a beam splitter.50% of the beam reflects to a lens of negative focal length which expands it.An iris then filters the beam which reaches the mirror placed left to the camera lens and illuminates the sample. Similarly, the rest 50% of the beam transmits to another mirror that reflects it to a negative lens. The beam is then filtered with an iris and reaches a mirror placed right to the camera lens and illuminates the sample. The

two mirros placed left and right from the camera lens ensure that the sample is illuminated homogeneously and shadow effects in projection data are weak.The flip mirror in figure 3.37 can switch from Argon-ion laser measurements to He-Ne laser measurements for each dye.

For the Alizarin Red S dye a 514 nm Argon-Ion laser was used to observe fluorescence. For Alcian-Blue dye, a 635nm He-Ne laser was used.For every dye the filters from section 3.81 table were placed in camera's lens in order to record signal from each dye.Exposure time is increased to 1second, and camera is thermoelectrically cooled down to -50°C .Projection recording step is 1°. In the next figures raw data measurements are represented along with the produced 3D volume for argon-ion laser and He-Ne Laser measurements respectively.Raw data shows the emission of Alcian Blue and Alizarin Red S.

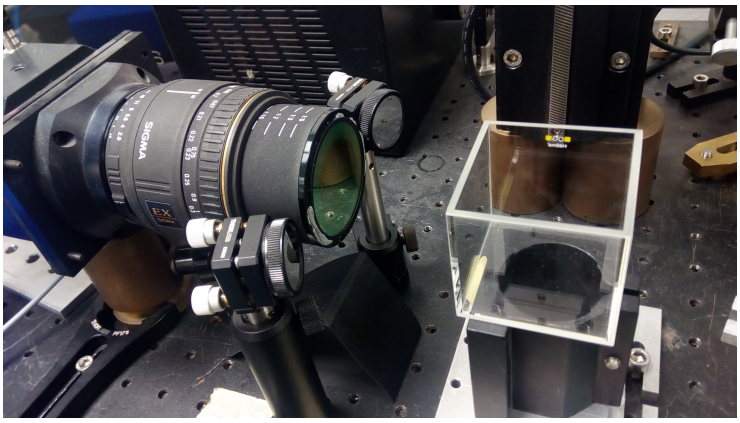

Figure 3.36: Experimental setup with water bath used for reflection measurements.

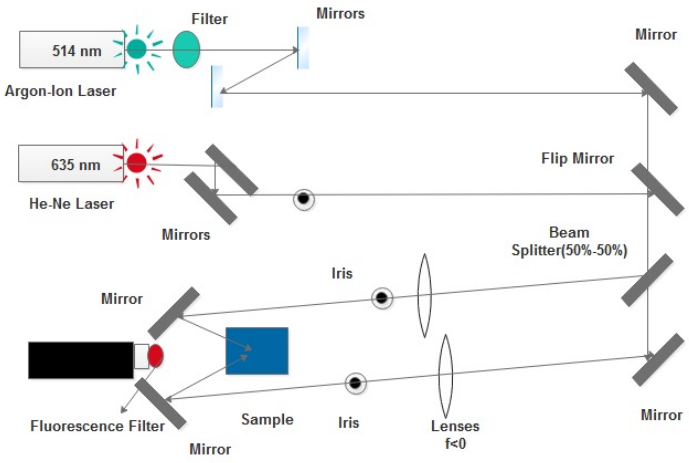

Figure 3.37: Experimental setup used for reflection measurements. [45]

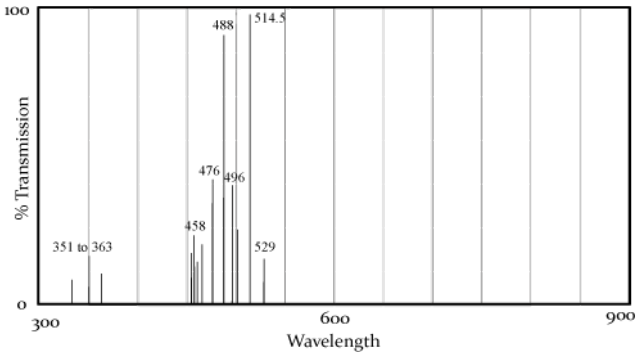

Figure 3.38: Argon ion Laser emission lines. A filter is used to transmit the 514nm line needed for the experiments. [36]

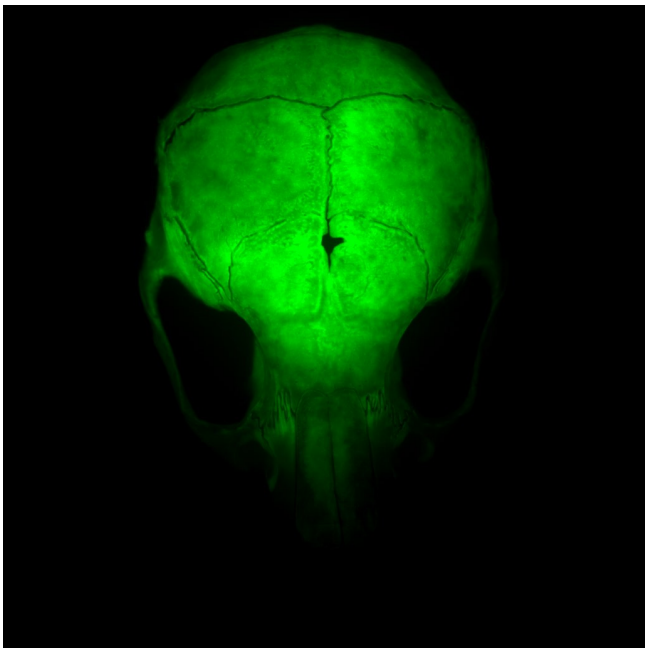

Figure 3.39: OPT data for Alizarin Red S

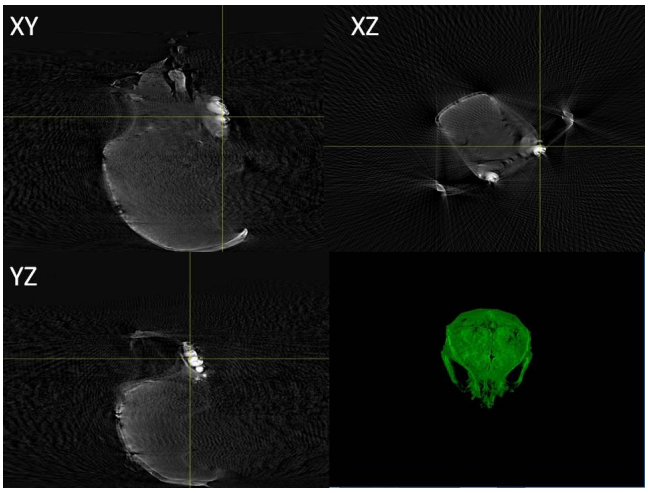

Figure 3.40: 3D Volume with XY,XZ,YZ Slices for Alizarin Red S fluorescence using 514nm Argon-Ion laser

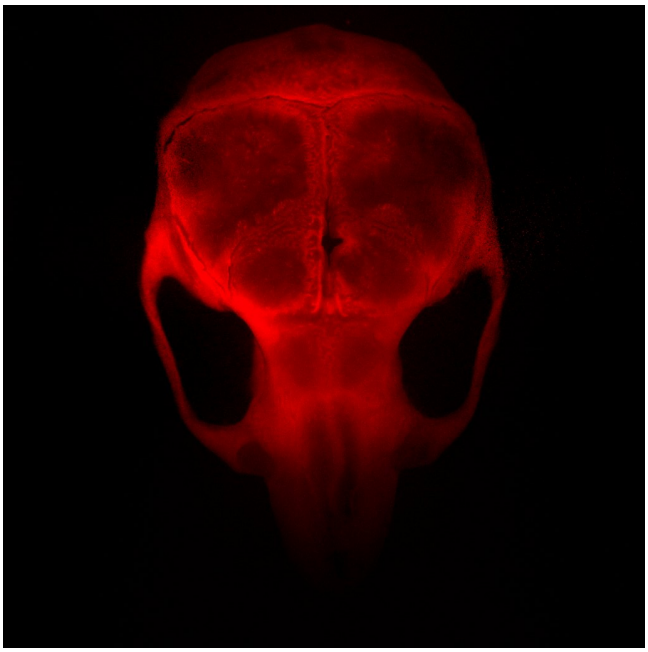

Figure 3.41: OPT Data for Alcian Blue

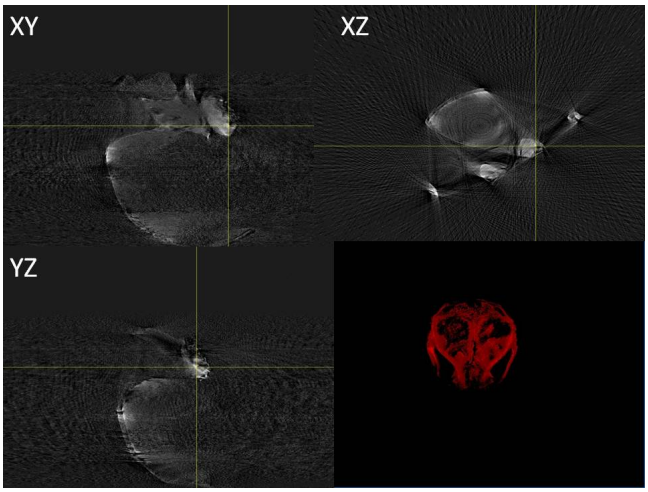

Figure 3.42: 3D Volume with XY,XZ,YZ Slices for Alcian Blue fluorescence using 514nm Argon-Ion laser

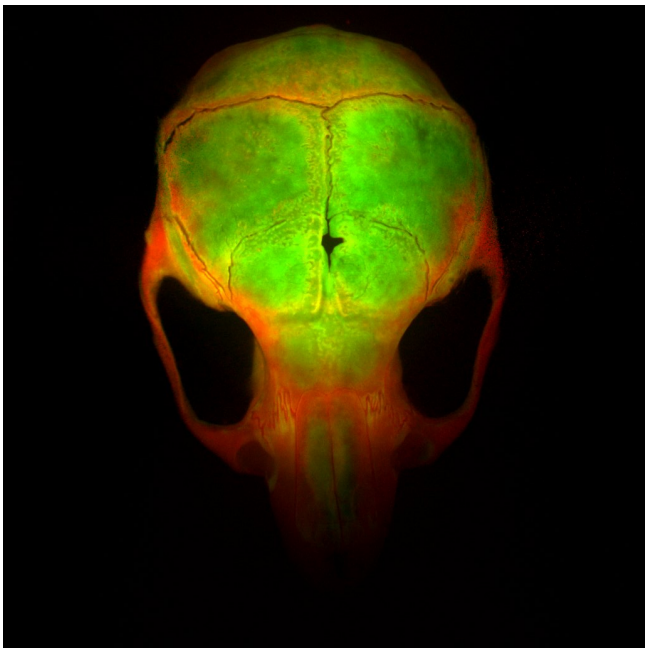

Figure 3.43: OPT Merged raw data for Alcian Blue and Alizarin Red S for 635 and 514nm laser measurements.

As seen from the previous images, fluorescence measurements can provide information about the specimen. Figure 3.43 with merged data can show which areas correspond to the bones of the skull and which areas correspond to cartilage. Fluorescence gave the abillity to image different parts of the skull using the dyes that it's painted with.Every dye emits in different areas of the skull.The OPT setup with these two possible geometries used can be used to give a more quantitative analysis for the measured samples.Reflection measurements can be used to map different areas of biological samples in order to obtain information from them.

3.10 Results

For the purpose of this project, a new geometry was developed for reflection measurements.Also, in order to measure the skull, a new protocol was created to load samples in OPT, which is why a new base was built to load the samples on the rotation stage of OPT. The transmission geometry provided information about absorption,so the 3D objects built from these measurements was a 3D map of the light attenuation of the sample. Reflection geometry was used for fluorescence measurements.3D objects built from these measurements were a 3D distribution map of the emission for each dye.The OPT setup gave 3D images

of the measured samples and provided more information about them.

3.11 Future Work

Future targets for the OPT is to further develop both Transmission and Reflection geometries while measuring various biological samples.Future use of the OPT could provide more quantitative analysis for the measured samples.Also, more testing could give fluorescence measurements using the transmission geometry ,something that could not be achieved for the purpose of this project,Finally, fluorescence could be used to obtain more information from the measured samples.

For the case of the skull, it was painted with these two dyes,so experiments showed the exact areas every dye emits light,something that was also clear with the 3D imaging of the skull.These conclusions can give room to further research while studying the evolution of a disease or maybe even test a possible treatment. The OPT setup is used for research evolving diabetes, melanomas and breast cancer. For instance, for the melanoma case, a mapping of the absorption can provide information whether a mark is malignant or not.Dosimetry experiments can also test various treatments.Optical Projection tomography, especially with the technology used in this project to examine samples, can be used for further analysis for several biological specimen and provide important information.

Bibliography

[1] X-Rays
https://en.wikipedia.org/wiki/X-rayl

[2] Crooke's Tube
https://en.wikipedia.org/wiki/Crookes_tube

[3] Joel D. Howel.l *Early clinical use of the X-ray.* Trans Am Clin Climatol Assoc, 127: 341–349, 2016

[4] Discovery of x-rays.
https://www.nde-ed.org/EducationResources/HighSchool/Radiography/discoveryxrays.html.

[5] Bremsstrahlung Radiation.
http://physicsopenlab.org/2017/08/02/bremsstrahlung-radiation/.

[6] Photoelectric effect.
https://www.britannica.com/science/photoelectric-effect.

[7] Photoelectric effect 2.
https://www.scienceabc.com/pure-sciences/what-explain-photoelectric-effect-einstein-definition-exmaple-applications-threshold-frequency.html.

[8] Photoelectric effect 3.
https://www.khanacademy.org/science/physics/quantum-physics/photons/a/photoelectric-effect.

[9] Photoelectric Effect 4 *Advanced physics lab guide* . E.Iliopoulos ,University of Crete ,Department of Physics,2013

[10] Compton Scattering
https://en.wikipedia.org/wiki/Compton_scattering

[11] X-ray attenuation.
http://www.spectroscopyonline.com/tutorial-attenuation-x-rays-matter.

[12] Raymond A. Serway , Clement J. Moses and Curt A. Moyer . *Modern Physics.*

[13] Avinash C. Kak, Malcolm Slaney. *Principles of Computerized Tomographic Imaging* . IEEE PRESS, 1987

[14] Gengsheng Lawrence Zeng *Medical Image Reconstruction, a conceptual tutorial* . Springer 2010

[15] Erika Garutti, Florian Grüner. *Lecture on Medical Physics* . 28/11/2014

[16] Radon Transform
https://www.youtube.com/watch?v=MA2y_2YySq0.

[17] Fourier Slice Theorem
https://www.youtube.com/watch?v=YIvTpW3IevI.

[18] Filtered Back Projection
https://www.youtube.com/watch?v=pZ7JlXagT0w.

[19] M.C Villa Uriol *Reconstruction from Projections* . Computational Imaging Lab

[20] Matlab's Radon Function
https://www.mathworks.com/help/images/ref/radon.html.

[21] Matlab's Inverse Radon Function
https://www.mathworks.com/help/images/ref/iradon.html.

[22] Jablonski Diagram
https://chem.libretexts.org/Textbook_Maps/Physical_and_Theoretical_Chemistry_Textbook_Maps/Supplemental_Modules_(Physical_and_Theoretical_Chemistry)/Spectroscopy/Electronic_Spectroscopy/Jablonski_diagram.

[23] Field of View
https://gamedev.stackexchange.com/questions/90448/what-is-fovx-in-this-diagram.

[24] Diaphragm
https://www.wildernessshots.com/how-to-use-f-stop-aperture/.

[25] Diaphragm
https://www.wildernessshots.com/how-to-use-f-stop-aperture/.

[26] Aperture,Depth of Field
https://www.howtobecomearockstarphotographer.com/basics-in-concert-photogprahy-i-aperture-shutter-speed-and-iso/ .

[27] Depth of Field
https://photographylife.com/what-is-depth-of-field.

[28] Sharpe J *Optical projection tomography.*. Annu Rev Biomed Eng. 2004;6:209-28.

[29] Athanasios Kokolakis,Giannis Zacharakis,Konstantin Krasagakis,Konstantinos Lasithiotakis,Rosy Favicchio,George Spiliopoulos,Elpida Giannikaki,Jorge Ripoll,Androniki Tosca *Prehistological evaluation of benign and malignant pigmented skin lesions with optical computed tomography.* Journal of Biomedical Optics 17(6),066004,June 2012

[30] Antonios E. Papadakis, Giannis Zacharakis, Thomas G. Maris, Jorge Ripoll and John Damilakis *A New Optical-CT Apparatus for 3-D Radiotherapy Dosimetry: Is Free Spacce Scanning Feasible?.* IEE transactions on medical imaging, vol29,no 5,may 2010

[31] A.E Papadakis, T.G Maris, G. Zacharakis, V. Papoytsaki, C. Varveris, J. Ripoll, J. Damilakis *Technical Note: A fast laser-biased optical-CT scanner for three dimensional radiation dosimetry.* Med. Phys. 38 (2), February 2011

[32] Optical Projection tomography
`https://www.jove.com/video/50238/near-infrared-optical-projection-tomography-for-assessments-cell-mass`.

[33] LEGO/ARDUINO Optical CT Scanner
`https://goo.gl/Mffb1m`.

[34] Desktop CT and 3D Scanner with Arduino
`https://www.instructables.com/id/Desktop-CT-and-3D-Scanner-With-Arduino/`.

[35] Fluorescence
`https://www.chroma.com/knowledge-resources`.

[36] Argon-Ion Laser Spectrum
`https://www.chroma.com/knowledge-resources/about-fluorescence/fluorescence-microscopy/light-sources`.

[37] Jens Fischbach, Qiuting Loh, F. F. Bier, Theam Soon Lim, Marcus Frohme, Jorn Glokler *Alizarin Red S for Online Pyrophosphate Detection Identified by a Rapid Screening Method* .

[38] Rahul Kaushika , Pawan Kumar, Amrita Ghosh Neha Guptab , Davinder Kaurc , Saroj Arorac and D. Amilan Jose *Alizarin Red S –Zinc(II) Fluorescent Ensemble For Selective Detection of Hydrogen Sulphide and Assay with H2S donor* .

[39] Alcian Blue 8 GS *https://www.serva.de/enDE/ProductDetails/72_12021_Alcian_Blue_8_GS_0_0.html* .

[40] Alcian Blue 8 GS *https://www.applichem.com/en/shop/product-detail/as/alcianblau-8-gs-ci-74240/* .

[41] W. Sabnis *Handbook of Biological Dyes and Stains: Synthesis and Industrial Applications* . Wiley,2010

[42] ,Mahendra Rai, Ph.D, Ranjita Shegokar, Ph.D *Metal Nanoparticles in Pharma* . Springer, 2017

[43] Rahul Kaushika , Pawan Kumar, Amrita Ghosh Neha Guptab , Davinder Kaurc , Saroj Arorac and D. Amilan Jose *Alizarin Red S –Zinc(II) Fluorescent Ensemble For Selective Detection of Hydrogen Sulphide and Assay with H2S donor* .

[44] David John Goldstein, Richard W. Horobin *Rate factors in staining by Alcian Blue* . The Histochemical Journal,1974

[45] Experimental Setup *Setup schemes done with Edraw Max software.*